

**OPTICAL INTERACTIONS IN A DIELECTRIC MATERIAL WITH
MULTIPLE PERTURBATIONS**

Thesis by

Hyuk Lee

**In Partial Fulfillment of the Requirements
for the Degree of
Doctor of Philosophy**

**California Institute of Technology
Pasadena, California**

1986

(Submitted December 9, 1985)

ACKNOWLEDGEMENTS

First and foremost it is a pleasure to acknowledge the guidance, and supervision of my advisor, Professor Demetri Psaltis.

I would like to thank Dr. Gabriel Sirat for helpful discussions in many areas.

Thanks are also due to my colleagues Dr. Eung Gi Paek, Kelvin Wagner, Mike Haney and John Hong with whom I discussed many subjects during my stay at Caltech.

Constant encouragement has come from my family.

ABSTRACT

The interaction of light propagating through a dielectric material with multiple perturbations is investigated.

A general coupled mode theory of two gratings is presented. The acousto-electro-optic effect is introduced as an example of an indirect interaction due to the acousto-optic and electro-optic effects. The acousto-electro-optic effect is analyzed using the general theory and is demonstrated experimentally. The application of this effect to light modulation and deflection is discussed in detail. Also a correlator that is based on the photorefractive acousto-electro-optic effect is demonstrated and analyzed theoretically.

TABLE OF CONTENTS

ACKNOWLEDGEMENTS	ii
ABSTRACT	iii
1.OVERVIEW	1
2. MULTIPLE PERTURBATIONS IN OPTICAL MATERIALS	
2.1. Perturbations of optical properties in materials	6
2.2. Significance of multiple perturbations in optical materials	12
3. COUPLED MODE THEORY	
3.1. Electric field coupled mode theory	16
3.2. Polarization of optical materials	17
3.3. Optical and acoustic eigenmodes of the unperturbed medium	23
3.3.1. Optical eigenmodes	23
3.3.2. Acoustic eigenmodes	27
3.4. Coupled mode equation of two gratings	29
3.5. Bandwidth of an acousto-optic device with a finite size transducer	32
4. HOMOGENEOUS ACOUSTO-ELECTRO-OPTIC EFFECT	
4.1. Acousto-electro-optic(AEO) interaction	40
4.2. Coupled mode analysis of the homogeneous AEO interaction	44
4.3. Experimental verification of the homogeneous AEO interaction	53

4.4. AEO modulator	65
4.5. AEO deflector	74
4.6. Novel way of measuring the acoustic transducer bandwidth	83
5. PHOTOREFRACTIVE AEO INTERACTION	
5.1. Spatial AEO interaction	85
5.2. Three-mode photorefractive AEO interaction	86
5.3. Experiment on photorefractive AEO interaction	92
5.4. Correlator using the intermodulation mode	99
6. FUTURE RESEARCH	106
REFERENCES	108

1. OVERVIEW

There are many different ways of perturbing the optical properties of materials. For example, we may launch acoustic waves to utilize the acousto-optic effect, or apply electric fields to change the index of refraction through the electro-optic effect. We may also consider the natural birefringence and optical activity inherent in some crystals as perturbations of the dielectric tensor.

In general, the macroscopic polarization of a material can be decomposed into components that are induced by different perturbations caused by external or internal agents. If two or more different sources of dielectric perturbation are present at the same time, the interaction between the incoming optical wave and the material is very nonlinear in the sense that the resulting field is not equal to the sum of the fields that would result from the individual perturbations. This introduces additional flexibility in controlling optical waves.

A general theory is needed to explore the full potentiality of optical interactions in materials with multiple perturbations. Coupled mode analysis is a powerful theoretical tool with which such higher interactions may be analyzed. We present a general

coupled mode theory for the interaction between multiple perturbations and optical waves. The theory is then used to study a phenomenon we refer to as the Acousto-Electro-Optic (AEO) interaction in crystals.

While the interactions known as the Acousto-Optic (AO) and the Electro-Optic (EO) effects have both been studied and used extensively, basic limitations in the performance of the devices utilizing such effects exist separately. When both AO and EO perturbations are applied simultaneously in a crystal, the combined effect (AEO) may be used to overcome some of the limitations inherent in the individual AO and EO devices.

As a first step, we studied the AEO effect with a spatially homogeneous electric field and a single frequency acoustic wave. The general theory was used to calculate the diffracted light intensity of the constant electric field AEO interaction as a function of the applied voltage. To verify the theory experimentally, an acousto-optic device with electrodes to apply the voltage was designed and fabricated. The experimental results verified the predicted dependence of the diffracted intensity on the applied voltage.

Based on the theoretical and experimental investigations of the AEO effect, a new one-dimensional spatial light modulator was devised. A new optical

deflector based on the AEO effect, called the AEO deflector, was also devised. This deflector can be described as a conventional AO deflector with the phase-mismatch compensated by the EO effect, resulting in an increase in the number of resolvable spots.

The capabilities of the AEO interaction can be exploited even further if a convenient method of applying a spatially varying electric field is available. An electric field grating can be created through yet another nonlinear interaction called the photorefractive effect, which is presently being investigated for applications in real-time holography. While the acoustic grating is dynamic and one-dimensional, the photorefractive grating is stationary and two-dimensional. This effect was studied theoretically and experimentally verified, demonstrating the applicability of the general theory to the analysis of complicated, multiple perturbation interactions. The intermodulation term that arises from the combined effect produces an output optical wave whose amplitude is the amplitude product of the two gratings. This product was used to construct a space-integrating correlator.

There are significant advantages to be gained by using multiple perturbation interactions in materials

for optical signal processing. In one crystal, many different input signals corresponding to the physical sources of the perturbations may be present, and the appropriate optical interaction may perform the desired computation on the inputs. Such advantages are clearly apparent in the AEO interaction. The study of more general types of interactions, those involving many material perturbations, should be pursued further. Another important subject for research is the study of the physical mechanisms of the interaction of optical waves and material perturbations. While effects such as the AEO effect arise from the interaction of optical waves with the sum of the material perturbations, direct coupling between the perturbations themselves may give rise to new effects arising from the interaction of optical waves with the product of the perturbations. The study of such new effects, interesting in its own right, may culminate in the invention of new devices for contribution in the field of optical signal processing.

In Chapter 2, we describe the general concept of the multiple perturbations of optical materials and the significance of the optical interaction of the multiple perturbations applied to optical signal processing and devices. The general coupled mode theory of two gratings is presented in Chapter 3. We will choose the simplest

example of an indirect interaction, the AEO interaction, and show how we can use this interaction to improve the functions of optical devices and to devise new devices in Chapters 4 and 5. These examples will demonstrate the potentiality of the general concept developed in Chapter 2.

A note on notation :

In this thesis the Einstein summation notation is used except when otherwise specified. Conventional arrow notation for a vector is used. Also component notation such as x_i is used for a vector \vec{x} .

2. MULTIPLE PERTURBATIONS IN OPTICAL MATERIALS

2.1. Perturbations of optical properties in materials

The fundamental equations which govern optical interaction with matter are Maxwell's equations and the material equations. In Maxwell's equations, optical waves are represented by electric and magnetic fields. The basic variables of the material are position vectors of molecules in classical physics, or wave functions of the material system in quantum physics. If there is no interaction between optical waves and matter, the fundamental equations consist of the free Maxwell and material equations. This means that there is no cross coupling between the two equations and we can solve them independently to get free optical waves and material system states. On the other hand, if there are interactions, Maxwell's equations and the material equations are coupled, and the two sets of variables which describe optical waves and materials appear in both equations.

The standard method of solving the coupled Maxwell and material equation is the so-called self-consistent analysis¹. In the self-consistent method we first obtain the response of the material to given electromagnetic fields. This response gives a constitutive relation for

the source term in Maxwell's equation, and then the wave equation is used to analyze the interaction of light with matter.

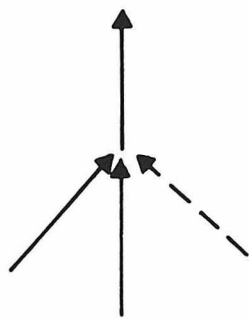
In the preceding discussion, we considered the material equation in general, but we did not specify external physical agents which can change the material states. As we have seen before, the material equation is coupled with Maxwell's equations. Therefore, if we change the material properties by external agents, the optical properties of the material change accordingly. This means that the constitutive relations are functions of all possible physical agents which affect states of the material as well as electric and magnetic fields. There are many different types of physical agents we can apply. Among these the acoustic displacement of molecules in the material is well known and important. The variable that characterizes the acoustic wave is the strain which measures displacements of molecules from their equilibrium positions. Also the electric and magnetic fields are commonly used external physical agents.

The magnitude of the change of the optical properties discussed above is usually small, implying that the terms in the power series expansion of the constitutive relation can be considered as

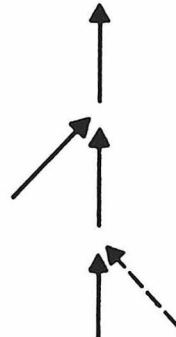
perturbations. Then we may call all physical agents that change optical properties of the material as perturbations. If there are many physical agents which simultaneously affect the optical properties of the material, we refer to these as multiple perturbations.

There are several types of interactions of light in a medium with multiple perturbations which can be categorized as follows. First we consider the direct interaction of multiple perturbations. Direct interaction can be characterized by an irreducible susceptibility that cannot be reduced to a product of lower-order interactions. The effect of a direct interaction becomes smaller as more perturbations are considered, and there is only one overall phase matching condition. We take acoustically induced optical harmonic generation (AIOHG)² as an example to illustrate the various types of interaction. In Fig.2.1.1(A) the wave vector diagram of the direct interaction of AIOHG is drawn. In this case the polarization is proportional to SE^2 , where S is the strain and E is the optical electric field. In contrast to the direct interaction, an induced interaction of multiple perturbations can be reduced to a composite of lower-order interactions. In this case we can write the susceptibility of the induced interaction as a product of lower-order

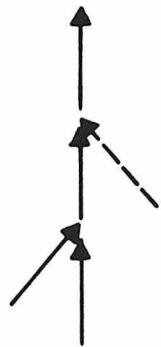
interaction susceptibilities; however, the polarization has the same form as that of the direct interaction. AIOHG can happen via not only induced interaction but also direct interaction. In Fig. 2.1.1(B),(C) two types of the induced AIOHG are drawn. We have the same input and output acoustic and optical waves as in Fig.2.1.1(A), but the interaction mechanism is different. The third interaction of multiple perturbations we refer to as the indirect interaction. An indirect interaction can be expressed as a sum of direct or induced interactions. In contrast to the indirect interaction, the direct or induced interactions can be attributed to one term in the power series expansion of the constitutive relation. As an example we draw the diagram corresponding to the indirect interaction for the AIOHG effect, which is represented by the polarization $SE + E^2$ in Fig. 2.1.1(D). The intermodulation of the indirect AIOHG effect may be represented by SE^2 ; however, to obtain large effect we need phasematching conditions separately for both interactions represented by the polarizations SE and E^2 . In this way the indirect interaction may be much stronger than the direct interaction. In this thesis we focus on indirect interactions.



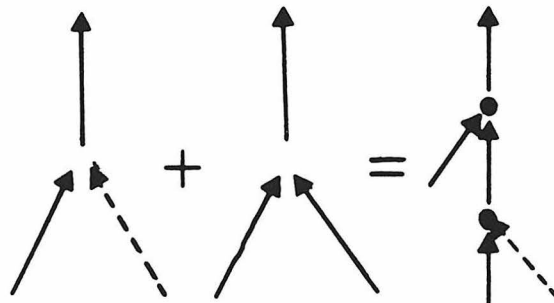
(A)



(B)



(C)



(D)

FIG 2.1.1

Fig 2.1.1 : Wave vector diagrams of examples of various optical interactions.

(a) Direct acoustically induced second harmonic generation(AIOHG).

(b),(c) Induced interaction of AIOHG.

(d) Indirect interaction of AIOHG. Two dots on the diagram implies phase matchings.

→ : Optical wave.

-----> : Acoustic wave.

2.2. Significance of multiple perturbations in optical materials

In Section 2.1, we introduced the concept of multiple perturbations and the interactions they induce inside optical materials. In this section, we discuss the significance between the interaction of multiple perturbations and optical signal processing and optical devices.

Optical signal processing systems and optical devices are based on intentional manipulations of optical waves which carry information to be processed. These manipulations are accomplished by selective physical interactions of optical waves and externally controlled physical agents(multiple perturbations) which contain information. From this consideration, we see the clear relation of interactions of multiple perturbations with the optical signal processing and optical devices. We need as many input signals as possible, which can be thought of multiple perturbations in the material, and we select the appropriate material and interaction to obtain the desired output result for the specific purpose of optical signal processing or optical device. This is the main motive of our investigation of interactions of multiple perturbations and optical waves.

The concept is illustrated in Fig.2.2.1. General input signals of the optical signal processing system or device may be an acoustic wave, electric fields provided by electrodes, magnetic fields or microwave, optical waves. We call these input signals as multiple perturbations that change the optical properties of the material. If we choose the correct material, orientation of the crystal cut and coupling geometry of multiple perturbations, the optical waves interact with multiple perturbations. It may be direct, indirect, induced or other types of interactions. Thus, the output optical waves or other types of perturbations are desired results of the optical signal processing and optical device. Ofcourse, we may need many different types of transducers to convert the information (for example, electrical) to perturbations of the material.

The indirect AEO effect³ is very interesting because of its flexibility and this is used to make new devices in Chapters 4 and 5.

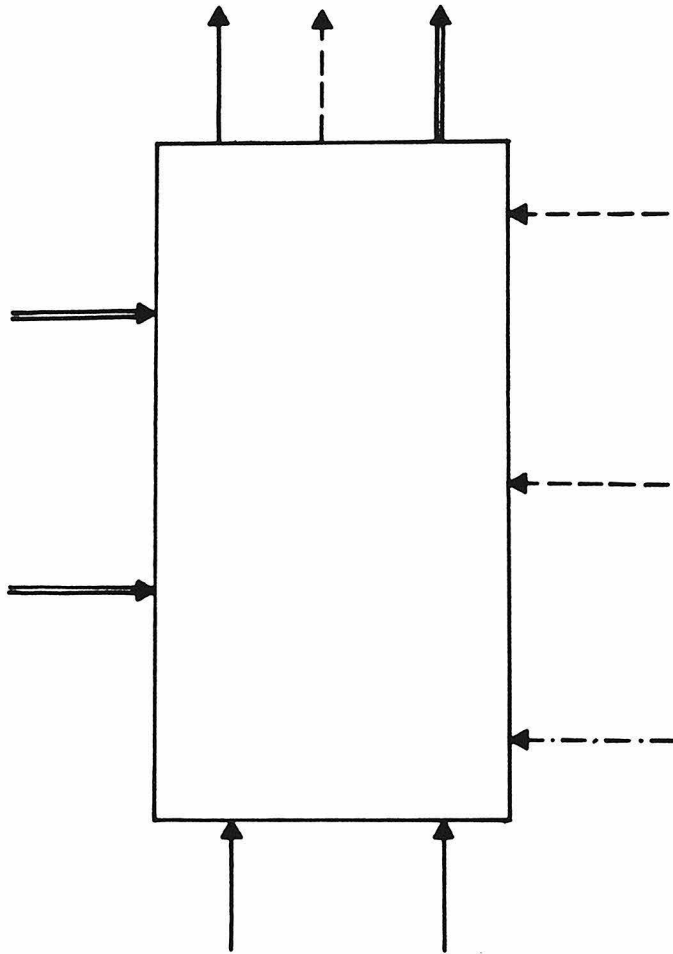


FIG 2.2.1

Fig 2.2.1: Illustration of the concept of the general optical interaction of multiple perturbations in dielectric materials.

→ : Optical wave.

⇒ : Acoustic wave.

-----> : Electric field.

-.-.-> : Other external physical agents.

3. COUPLED MODE THEORY

3.1. Electric field coupled mode theory

Coupled mode theory is a well-known method which has been used in solving problems of nonlinear optics, acousto-optics and other differential equations with perturbations. In this thesis we use coupled mode analysis to characterize interactions due to multiple perturbations. In this section we compare various coupled mode theories for the acousto-optic interaction. Acousto-optic interaction is an interaction between acoustic and optical waves, and it will be explained in detail in Section 4.1. There have been many papers analyzing this effect. In the review paper by I.C.Chang⁴ in 1976, he used a scalar coupled mode equation of electric field amplitudes. J.M.Rouaven et al.⁵ used correct electric displacement eigenmodes to analyze the acousto-optic interaction; however, they did not include the expression for the final diffracted light intensity, since it is not convenient to get this intensity from the electric displacement vectors. In this thesis we use electric field eigenmode expansions which are not an orthonormal set in an anisotropic medium but can be decoupled, as we will see. The use of electric field is preferable because it is the physical

quantity that is of importance and not the electric displacement vector. Also the simplest expression for the intensity of the diffracted light is given when we use the electric field.

In this chapter we develop this electric field coupled-mode theory for the simple case of two gratings, which is the simplest example of multiple interactions and is also useful in the analysis of the AEO interaction.

3.2. Polarization of optical materials

Optical materials respond to applied external perturbations in various ways. In general, these interactions can be categorized as linear or nonlinear responses. The interaction is defined to be linear if the induced macroscopic polarization is proportional to the optical wave. Examples are natural birefringence, optical activity and also the acousto-optic and electro-optic effects.

One way of expressing the response of the material is to use macroscopic polarization. We can expand the macroscopic polarization of the optical material into products of external multiple perturbations. Also the response is expressed as a change in the relative inverse dielectric tensor. In this section we use both

definitions. Thus, we need the relation which connects these two definitions. The definition of the change of polarization and relative dielectric tensor is given by:

$$\Delta P_i = \epsilon_0 (\Delta \epsilon)_{ij} E_j, \quad (3.2.1)$$

where ϵ_0 is the dielectric constant in vacuum and $(\Delta \epsilon)_{ij}$ is the relative dielectric tensor. If the perturbation is small, to first order, a change in the relative inverse dielectric tensor is related to a change in the relative dielectric tensor by :

$$\Delta \epsilon_{ij} = - \epsilon_{ik} \epsilon_{jl} (\Delta \epsilon^{-1})_{kl}, \quad (3.2.2)$$

where ϵ_{ik} is the relative dielectric tensor for the unperturbed medium. If we use (3.2.1) and (3.2.2), we have :

$$\Delta P_i = - \epsilon_0 \epsilon_{ik} \epsilon_{jl} (\Delta \epsilon^{-1})_{kl} E_j. \quad (3.2.3)$$

Natural birefringence is a simple linear interaction. It is very important because of its critical contribution to other interactions as will be seen in later sections. For the case of monochromatic light, we can define the overall relative dielectric tensor of natural birefringence, which is the

characteristic constant of the unperturbed medium, as :

$$\epsilon_{ij} = \delta_{ij} + 4\pi k_{ij}, \quad (3.2.4)$$

where δ_{ij} is the Kroneker delta and k_{ij} is the natural relative dielectric susceptibility.

Another linear response of the material that is important for our work is the linear electro-optic effect. This interaction comes from the quadratic term of the expansion of the polarization into electric fields. The linear electro-optic effect is defined as the change of the inverse relative dielectric tensor :

$$(\Delta \epsilon^{-1})_{ij} = r_{ijk} E_k^{(ext)}, \quad (3.2.5)$$

where r_{ijk} is the linear electro-optic coefficient and $E_k^{(ext)}$ is the applied external electric field which may be constant, or temporally or spatially varying. We treat different cases of linear electro-optic effects in later sections.

The acousto-optic interaction may be explained intuitively as follows. If we launch an acoustic wave inside the crystal, we create a density change, and this alters the optical property, (i.e., polarization) locally. We know that given a grating we can diffract the light; thus, the acousto-optic interaction couples the density grating of the crystal and the optical wave.

The definition of this interaction is given by :

$$(\Delta\epsilon^{-1})_{ij} = p_{ijkl}S_{kl}, \quad (3.2.6)$$

where p_{ijkl} is the fourth rank elasto-optic tensor and S_{kl} is the strain induced by the acoustic field inside the crystal. The strain is defined as :

$$S_{kl} = 1/2 [D_k(u_l) + D_l(u_k)], \quad (3.2.7)$$

where u_l is the displacement vector field of material points of the crystal, and D_k is a partial differential operator with respect to x_k . As we see in (3.2.6), p_{ijkl} is dimensionless and has the following symmetry property :

$$p_{ijkl} = p_{jikl} = p_{ijlk}. \quad (3.2.8)$$

This is the direct acousto-optic interaction. For a piezo-electric crystal, i.e., a crystal that changes polarization when a strain is applied, the combined piezo-electric and linear electro-optic interactions give an indirect acousto-optic effect. This interaction is :

$$(\Delta P)_i = -\epsilon_0 [(2b_{ijm} s_m s_n e_{nkl}) / (s_p \epsilon_{pq} s_q)] E_j S_{kl}, \quad (3.2.9)$$

where s_i is the i^{th} component of a unit vector in the direction of light propagation, b_{ijm} is the optical

mixing susceptibility and e_{nkl} is the piezo-electric stress tensor. The direct and indirect acousto-optic interactions described above depend only on the strain. Nelson and Lazay⁶ showed that actually the acousto-optic interaction depends also on the rotation. This effect is generally very small but it can, under proper conditions, be large. If we include this interaction, the complete expression of the acousto-optic effect is given by :

$$\Delta P_i = -\epsilon_0 [\epsilon_{im} \epsilon_{jn} D_{mnkl} + (\epsilon_{i[k} \delta_{l]j} + \epsilon_{j[k} \delta_{l]i}) + (2b_{ijm} s_m s_n e_{nkl}) / (s_p \epsilon_{pq} s_q)] E_j D_l(u_k). \quad (3.2.10)$$

Another effect that is important to our work is optical activity. This is an intrinsic property of the crystal, and it is difficult to change this property by applying external perturbations. However, recently liquid crystals or organic materials are being investigated to get large nonlinear coupling coefficients. In this case we can change the optical activity externally, in which case it can be treated using coupled mode analysis in a manner analogous to the way in which acoustic or electric field gratings are treated mathematically. Optical activity is written as a perturbation of the dielectric tensor as follows :

$$\epsilon_{ij} = \delta_{ij} + 4\pi k_{ij} + j \epsilon_{ijl} g_{lm} s_m, \quad (3.2.11)$$

where $j = (-1)^{1/2}$, ϵ_{ijl} is the complete antisymmetric tensor, g_{lm} is the gyration tensor and s_m is the m^{th} component of the unit vector in the direction of the optical wave.

Summarizing the above discussion, we use (3.2.11) as the relative dielectric tensor for the unperturbed medium with which we derive plane wave eigenmodes to be used in expanding the solution of the perturbed interaction. Next, the perturbation in the polarization introduced by simultaneous application of multiple perturbations is given by :

$$(\Delta P_i)_{\text{tot}} = \sum_{\mathbf{b}} a_{ij}^{(\mathbf{b})} E_j, \quad (3.2.12)$$

where \mathbf{b} represents all the perturbations.

This is the fundamental relation for our work and we use this equation in Chapters 4 and 5 to treat the acousto-electro-optic effect.

In this section we focused primarily on acousto-optic and linear electro-optic interactions. But there are many higher-order nonlinearities which are very interesting to future research work. For example, nonlinearities represented by SE^2 or S^2E terms in the expansion of the polarization can be very interesting. These nonlinearities are especially important in the case of surface acoustic waves because of the high

acoustic energy density.

3.3. Optical and acoustic eigenmodes of the unperturbed medium

In Section 3.2, we discussed various polarization changes of the crystal. Usually the effects of these interactions is very small, and can be treated as perturbations. This observation allows us to use in general a perturbative expansion of the solution describing this interaction. In the perturbative expansion, we need a complete set of eigenmodes of the unperturbed medium as a zero-order solution. In this section we first characterize optical eigenmodes and secondly, acoustic eigenmodes, which will be useful for the analysis of the acousto-electro-optic interaction.

3.3.1. Optical eigenmodes

Optical wave propagation can be explained using Maxwell's equations. Maxwell's equations for a charge-free nonmagnetic material in the MKSA unit system is given by :

$$\text{Div}(\vec{Y})=0 \quad \text{Div}(\vec{E})=0 \quad (3.3.1.1)$$

$$\text{Curl}(\vec{E}) + D_t(\vec{B}) = 0 \quad \text{Curl}(\vec{H}) - D_t(\vec{Y}) = 0 \quad (3.3.1.2)$$

$$\vec{Y} = \epsilon_0 \epsilon \vec{E} \quad \vec{B} = \mu_0 \vec{H}, \quad (3.3.1.3)$$

where ϵ_0 is the dielectric constant in vacuum, ϵ is the relative dielectric tensor which has been discussed in Section 3.2, and \vec{Y} is the displacement vector. We assume that ϵ is a hermitian tensor since we will treat nonabsorbing materials. In this case the free charge density is zero, and the relative dielectric tensor should be hermitian. If ϵ is a constant Hermitian tensor, then we obtain a set of infinite plane monochromatic waves as solutions of the free Maxwell wave equation. Let the plane wave propagate in the s direction. We can write this wave as :

$$E_1^{(p)} = E^{(p)} e_1^{(p)} \exp[j\omega\{(n^{(p)}x_i s_i/c) - t\}] \quad (3.3.1.4)$$

$$Y_1^{(p)} = Y^{(p)} d_1^{(p)} \exp[j\omega\{(n^{(p)}x_i s_i/c) - t\}], \quad (3.3.1.5)$$

where $p = 1, 2$ is an index used to distinguish the two different transverse polarizations, ω is the optical frequency, c is the speed of light in vacuum, $n^{(p)}$ are indices of refraction and $e_1^{(p)}$ and $d_1^{(p)}$ are unit dimensionless vectors in the direction of the eigenvectors. From (3.3.1.2) and (3.3.1.3), we obtain the well-known Maxwell wave equation :

$$D_k D_k (E_1) - D_k (D_1 (E_k)) = (1/c^2) D_t^2 (\epsilon_{1m} E_m). \quad (3.3.1.6)$$

To get the relations between $e_l^{(p)}$ and $n^{(p)}$, we substitute (3.3.1.4) into (3.3.1.6). We wind up with the following equation :

$$(\delta_{lm} - s_l s_m) e_m^{(p)} = (n^{(p)})^{-2} (\epsilon_{lm} e_m^{(p)}). \quad (3.3.1.7)$$

From (3.3.1.7) the indices of refraction $n^{(p)}$ can be found from the condition that a nontrivial solution of the homogeneous equations exists. Then for each value of the index of refraction, the eigenvectors $e_m^{(p)}$ satisfy (3.3.1.7). Until now we have used electric field vectors to get electric field eigenmodes. It is well known that in an anisotropic medium the electric field eigenvectors are not orthogonal to each other. If we use electric displacement vectors, the eigenvectors are indeed orthogonal. So we use two sets of eigenmodes generally. Maxwell's wave equation for the displacement vectors is given by :

$$\begin{aligned} D_k D_k [(\epsilon^{-1})_{lm} Y_m] - D_k (D_l [(\epsilon^{-1})_{km} Y_m]) \\ = (1/c^2) D_t^2 (Y_l). \end{aligned} \quad (3.3.1.8)$$

If we substitute (3.3.1.5) into (3.3.1.8), we get :

$$\begin{aligned} [(\epsilon)^{-1}_{lm} - (\epsilon)^{-1}_{km} s_k s_l] d_m^{(p)} \\ = (n^{(p)})^{-2} d_l^{(p)}. \end{aligned} \quad (3.3.1.9)$$

We are now in a position to derive various conditions

for the eigenvectors $e_1^{(p)}$ and $d_1^{(p)}$. First we defined $e_1^{(p)}$ and $d_1^{(p)}$ to be unit vectors. This gives :

$$e_1^{(p)} e_1^{(p)*} = d_1^{(p)} d_1^{(p)*} = 1. \quad (3.3.1.10)$$

Next, if we use the first part of (3.3.1.1) and (3.3.1.5), we get the transversality condition of $d_1^{(p)}$:

$$d_1^{(p)} s_1 = 0 \quad p = 1, 2. \quad (3.3.1.11)$$

The orthogonality relation between $d_1^{(1)}$ and $d_1^{(2)}$ comes from (3.3.1.9), using the relation (3.3.1.11) and Hermiticity of the tensor ϵ_{1m} :

$$d_1^{(1)} d_1^{(2)*} = 0. \quad (3.3.1.12)$$

If we apply the same method used above and use the orthogonality relation between $d_1^{(1)}$ and $d_1^{(2)}$, we get the following relation :

$$d_1^{(1)} e_1^{(2)*} = d_1^{(2)} e_1^{(1)*} = 0. \quad (3.3.1.13)$$

It may now be apparent why we use two sets of eigenvectors. We like electric field eigenmodes but we use electric displacement eigenmodes to decouple the polarizations. Relations (3.3.1.10), (3.3.1.11), (3.3.1.12) and (3.3.1.13) with eigenmode equations (3.3.1.4), (3.3.1.5) will be used to derive the coupled mode equation.

The above method of getting eigenmodes is very general because it applies to any kind of constant Hermitian dielectric tensor, and this sort of generality is important, when we use a computer to design actual devices. Homogeneous perturbations can be thought as part of the unperturbed dielectric tensor. On the other hand, we can also think of the constant change of the dielectric tensor as a small perturbation. This gives rise to combined interactions of homogeneous perturbations and other effects. This point will be discussed in Chapters 4 and 5.

3.3.2. Acoustic eigenmodes

The response of a material to applied strain obeys Hooke's law. Hooke's law gives a relation between stress and strain :

$$T_{ij} = c_{ijkl}S_{kl}, \quad (3.3.2.1)$$

where T_{ij} is the stress and c_{ijkl} is the elastic stiffness tensor. The equation of motion for the displacement vectors of material points u_i is given by :

$$\rho D_t^2 u_i = D_j T_{ij}, \quad (3.3.2.2)$$

where ρ is the mass density of the material. Let us assume a plane acoustic wave with a frequency Ω and

propagating in the direction N_i :

$$u_i^{(a)} = U_i^{(a)} \exp[j(\Omega x_1 N_1 / V_a - \Omega t)]$$

$$a=1,2,3 , \quad (3.3.2.3)$$

where $U_i^{(a)}$ are constant.

If we substitute (3.3.2.3) into (3.3.2.2), we get a system of linear equations which give phase velocities V_a and eigenvectors $U_i^{(a)}$:

$$[\rho(V_a)^2 \delta_{ik} - c_{ijkl} N_j N_l] U_k^{(a)} = 0. \quad (3.3.2.4)$$

From (3.3.2.4), we see that there are three different eigenmodes for a given direction N_i , and in general these eigenmodes are mixed, i.e., not pure transverse or longitudinal. Many crystals we are using are piezoelectric. This piezoelectricity changes the elastic stiffness tensor because it generates stress induced by the electric field. In this case the effective stress tensor is given by :

$$T_{ij} = c_{ijkl} S_{kl} - e_{kij} E_k. \quad (3.3.2.5)$$

3.4. Coupled mode equation of two gratings

The simplest case of multiple gratings is two gratings. In this section, we introduce the coupled mode equation of two gratings and discuss approximations to be used for the calculation of the AEO effect. Also the interaction of an incident beam with two gratings is of practical importance in devices such as an AO modulator.

The wave equation that governs the interaction of the optical wave with multiple perturbations is :

$$D_k D_k (E_l) - D_k (D_l (E_k)) = c^{-2} D_t^2 (\epsilon_{lm} E_m). \quad (3.4.1)$$

The total relative dielectric tensor is taken to be the sum of two perturbations :

$$\epsilon_{ij} = \epsilon_{ij}^{(0)} + \Delta \epsilon_{ij}^{(1)} + \Delta \epsilon_{ij}^{(2)}. \quad (3.4.2)$$

In (3.4.2), two perturbations may be purely acoustic or acousto-electro-optic, i.e., acoustic and electro-optic gratings. Usually we assume plane monochromatic gratings for $\Delta \epsilon_{ij}^{(1)}$ and $\Delta \epsilon_{ij}^{(2)}$:

$$\begin{aligned} \epsilon_{ij} = & 1/2 \epsilon_{ij}^{(0)} + 1/2 a_{ij}^{(1)} \exp[j(\Omega^{(1)} t - K_1^{(1)} x_1)] \\ & + 1/2 a_{ij}^{(2)} \exp[j(\Omega^{(2)} t - K_1^{(2)} x_1)] + c.c. , \end{aligned} \quad (3.4.3)$$

where $\Omega^{(1)}$ and $\Omega^{(2)}$ are temporal frequencies of the two gratings, $K_1^{(1)}$ and $K_1^{(2)}$ are the corresponding wave

vectors. Next we assume a plane monochromatic optical wave with unit amplitude incident on the crystal :

$$\begin{aligned} E_i^{(0,0,1)} \\ = e_i^{(0,0,1)} \exp[j\{((\omega n^{(0,0,1)})/c)s_1 x_1 - \omega t\}], \end{aligned} \quad (3.4.4)$$

where 1 in (0,0,1) represents the polarization of the input optical wave. We define various quantities which represent higher order modes :

$$\omega^{(I,J)} = \omega + I\Omega^{(1)} + J\Omega^{(2)} \quad (3.4.5)$$

$$X_i^{(I,J)} = \omega n^{(0,0,1)} s_i / c + IK_i^{(1)} + JK_i^{(2)} \quad (3.4.6)$$

$$s_i^{(I,J)} = X_i^{(I,J)} / |\vec{X}^{(I,J)}| \quad (3.4.7)$$

$$k_i^{(I,J,p)} = \omega^{(I,J)} n^{(I,J,p)} s_i^{(I,J)} / c \quad (3.4.8)$$

$$u^{(I,J)} = x_i s_i^{(I,J)}, \quad (3.4.9)$$

where I,J are integers.

The trial solution for the electric field for the two gratings case is given by :

$$\begin{aligned} E_i(x,t) = [F^{(I,J,p)}(u^{(I,J)})(n^{(I,J,p)})^{-1/2}] e_i^{(I,J,p)} \\ \times \exp[j(k_1^{(I,J,p)} x_1 - \omega^{(I,J)} t)]. \end{aligned} \quad (3.4.10)$$

Here we used normalized slowly varying amplitudes $F^{(I,J,p)}$ which give simple expressions for the diffracted light intensities. Next the phase mismatch

vectors for two gratings are :

$$\Delta k_1^{(I,J,p)} = k_1^{(I,J,p)} - x_1^{(I,J)}. \quad (3.4.11)$$

We now use the following adiabatic condition :

$$|(\dot{d}^{(I,J)})^2 F^{(I,J,p)}| \ll [2\omega^{(I,J)} n^{(I,J,p)} / c] |d^{(I,J)} F^{(I,J,p)}|. \quad (3.4.12)$$

Next we substitute the trial solution (3.4.10) into the wave equation (3.4.1) and use the properties of the eigenmodes described in section 3.3 and approximations (3.4.12). Then we get the coupled mode equation for two gratings :

$$\begin{aligned} & d^{(I,J)} F^{(I,J,q)} \\ &= K_+(I,J,q,p,1) F^{(I+1,J,p)} \exp[j(\Delta k^{(I+1,J,p)} - \Delta k^{(I,J,q)})_r] \\ &+ K_-(I,J,q,p,1) F^{(I-1,J,p)} \exp[j(\Delta k^{(I-1,J,p)} - \Delta k^{(I,J,q)})_r] \\ &+ K_+(I,J,q,p,2) F^{(I,J+1,p)} \exp[j(\Delta k^{(I,J+1,p)} - \Delta k^{(I,J,q)})_r] \\ &+ K_-(I,J,q,p,2) F^{(I,J-1,p)} \exp[j(\Delta k^{(I,J-1,p)} - \Delta k^{(I,J,q)})_r], \end{aligned} \quad (3.4.13)$$

where $r = s_i x_i$.

Temporal frequencies of acoustic waves or electric signals are small compared with that of the optical wave. This allows us to use ω instead of $\omega^{(I,J)}$ in (3.4.13). Of course, practical ranges of I,J are small. Next constant perturbations which give rise to the

anisotropy of the material are very small. And the difference between electric field eigenvectors $e_1^{(I,J,p)}$ and electric displacement eigenvectors $d_1^{(I,J,p)}$ are linear in the magnitude of the perturbation. So we can use $e_1^{(I,J,p)}$ at any place. If we assume that the magnitude of the wave vectors of the gratings is small we can use $u^{(0,0)}$ instead of $u^{(I,J)}$. One more approximation is applied to the approximate formula of the light intensity of the plane optical wave. The intensity is taken as the modulus square of the electric field. Given the initial conditions, we can easily solve the above coupled equation. The light intensity for each mode of order (I,J,p) is given by :

$$I_d = I_{in} |F^{(I,J,p)}|^2. \quad (3.4.14)$$

3.5. Bandwidth of an acousto-optic device with a finite size transducer

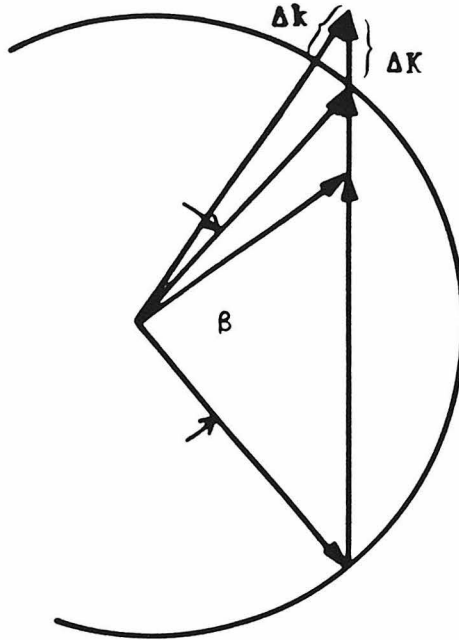
In this section we apply the coupled mode equations derived in Section 3.4 to the problem of calculating the bandwidth of the acousto-optic device. The input electrical signal fed into the AO device consists of a range of frequencies. The center frequency of the signal is chosen for the specific AO device, and the angle of

the illuminating beam is set to give zero phase mismatch for the center frequency. Thus, there are many different acoustic gratings with different wave numbers inside the crystal of the AO device. We can observe harmonic or intermodulation modes for all acoustic gratings. Also, the finite size of the transducer or crystal gives rise to angular spectral components of the acoustic wave propagating inside the crystal. Then we can expand the acoustic wave into a sum of acoustic angular eigenmodes.

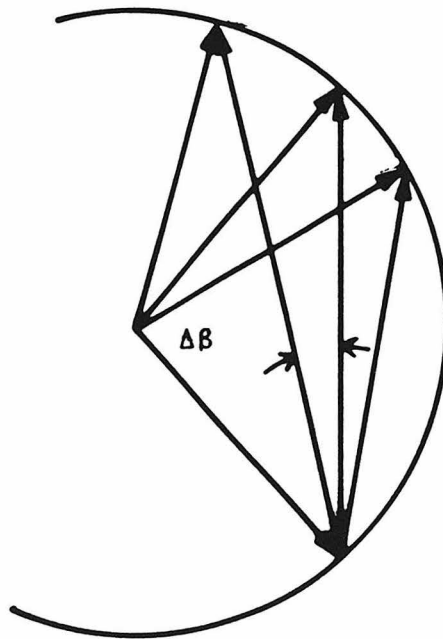
One of the fundamental parameters of the AO device is the bandwidth. Due to the phasemismatch introduced by the deviation from the center frequency, the amplitude of the output diffracted optical wave becomes smaller as the frequency goes away from the center frequency. This determines the useful frequency range or the bandwidth of the device. As an example, the bandwidth defined above can be calculated as in Fig.3.5.1(a) for isotropic diffraction. Here we neglect harmonic or intermodulation modes. In Fig.3.5.1(a), the frequency deviation from the center frequency is introduced by ΔK and the phasemismatch is called Δk . From the diagram in Fig.3.5.1(a), we have :

$$\Delta k = k - \{k^2 + [2k\sin(\beta/2) - \Delta K]^2 - 2k[2k\sin(\beta/2) - \Delta K]\cos(\pi/2 - \beta/2)\}^{1/2}, \quad (3.5.1)$$

34



(a)



(b)

FIG 3.5.1

Fig 3.5.1 : Wave vector diagram used in deriving formulae for the bandwidth.

(a) Derivation based on the phase mismatch.

(b) Derivation based on the finite size of the transducer.

where $k = 2\pi n/\lambda$: optical wave length in a crystal, n : index of refraction of the crystal, β : Bragg angle for the center frequency.

We assume $\Delta K/k \ll 1$. This is true because the wave length of the acoustic wave is much larger than that of the optical wave. Then the phasemismatch in (3.5.1) is approximated as :

$$\Delta k \sim \Delta K \sin(\beta/2). \quad (3.5.2)$$

We also have a relation between the frequency deviation $\Delta\Omega$ and ΔK :

$$\Delta K = \Delta\Omega / V_a, \quad (3.5.3)$$

where V_a is the acoustic velocity.

The well-known formula for the AO diffracted light intensity is given by :

$$I_d = I_{in} \eta [\text{sinc}(\Delta k L / 2)]^2, \quad (3.5.4)$$

where η is the diffraction efficiency for the center frequency, L is the interaction length and $\text{sinc}(x) = (\sin(x))/x$. From (3.5.4), the first zero of the diffracted light intensity is given by :

$$\Delta k L / 2 = \pi. \quad (3.5.5)$$

Using (3.5.2), the bandwidth is given by :

$$\Delta K = 2\pi/[L\sin(\beta/2)]. \quad (3.5.6)$$

Another way of defining the bandwidth that is related to the subject matter of this thesis is shown in Fig.3.5.1(b). Due to the finite size of the transducer or the crystal for a given acoustic frequency, we have acoustic waves over an angular spectrum. Then, for a frequency deviation ΔK , we can find an angle $\Delta\beta_a$ which gives exact phase matching. Only this phasematched component is nonzero because the interaction length is infinite and it results from the equation (3.4.13). In this case the amplitude of the acoustic wave is smaller than that of the center frequency. This reduces the diffracted light intensity and gives rise to the bandwidth of the device. $\Delta\beta_a$ is the spread angle which gives exact phasematching. Simple trigonometry applied in the diagram in Fig.3.5.1(b) gives :

$$2k\cos(\pi/2 - \beta/2 - \Delta\beta_a) = 2k\sin(\beta/2) + \Delta K. \quad (3.5.7)$$

As in the above, if we assume :

$$\Delta\beta_a \ll \beta/2, \quad (3.5.8)$$

we get the approximate expression of $\Delta\beta_a$:

$$\Delta\beta_a \sim \Delta K/[2k\cos(\beta/2)]. \quad (3.5.9)$$

If the size of the transducer is T , the angular spectrum is given by :

$$A_a \sim \text{sinc}(\pi \Delta \beta_a T / W), \quad (3.5.10)$$

where W is the wavelength of the acoustic wave.

So the first zero of the angular spectrum is :

$$\Delta \beta_a = W / T, \quad (3.5.11)$$

And the bandwidth follows from (3.5.9) :

$$\Delta K = 2k \cos(\beta/2) (W/T). \quad (3.5.12)$$

Now we have two definitions for the bandwidth. But they are same as can be shown as follows. From (3.5.12):

$$\Delta K = [2k \sin(\beta/2) / \sin(\beta/2)] [W \cos(\beta/2) / T]. \quad (3.5.13)$$

If we use the Bragg condition, (3.5.13) becomes :

$$\begin{aligned} \Delta K &= [KW / \sin(\beta/2)] [\cos(\beta/2) / T] \\ &= [2\pi / \sin(\beta/2)] [\cos(\beta/2) / T]. \end{aligned} \quad (3.5.14)$$

Next from the simple trigonometry , the relation between L and T is given by :

$$L \cos(\beta/2) = T. \quad (3.5.15)$$

Using this relation in (3.5.14), we get :

$$\Delta K = [2\pi / L] [1 / \sin(\beta/2)]. \quad (3.5.16)$$

This is exactly the same as (3.5.6). This shows that we can calculate the bandwidth in either way described above. The latter method of calculating the bandwidth is more advantageous than the other method if we consider the case of acoustic anisotropy.

4. HOMOGENEOUS ACOUSTO-ELECTRO-OPTIC EFFECT

4.1. Acousto-electro-optic(AEO) interaction

We described the general idea of multiple perturbations in optical materials, and the general concept of optical signal processing and devices in Chapter 2. Also, we developed coupled mode equations which can be used to analyze the combined interaction of multiple perturbations theoretically. In the following two chapters, we take a specific combined interaction, i.e., AEO interaction, to demonstrate the usefulness of the concepts developed.

The AEO interaction is a combined effect of AO and EO interactions. These two effects have been known for a long time, and used extensively for many types of optical devices, such as modulator, deflector, filter, etc.. Thus these individual effects have been analyzed theoretically by many authors. Our motive to investigate the AEO interaction was that, if we use both AO and EO effects, we may have more flexibility in making better devices. The limitations of each AO and EO device are well known. So we may improve functions of devices using both interactions. Examples of this idea will be given in Sections 4.4 and 4.5.

The commonly used AO device is based on travelling

acoustic waves. On the other hand, both temporally and spatially varying electric fields have been used for EO devices. Homogeneous AEO interaction is represented by the sum of the polarization induced by the travelling acoustic wave and the homogeneous electric field.

The theoretical tool we use to analyze the homogeneous AEO interaction is the general coupled mode equation for two gratings. In this case, only the acoustic wave is a grating, whereas the homogeneous electric field gives rise to a homogeneous perturbation via the linear electro-optic effect. There are two ways of analyzing the homogeneous AEO interaction. First, we may treat AO and EO effects as two perturbations. In this case, we can use the general coupled mode equation developed in the previous chapter. On the other hand, we may include the homogeneous perturbation induced by the constant electric field in the unperturbed dielectric tensor of the material. The effect of the homogeneous EO interaction is to change the index of refraction of the material of the conventional AO device. This interpretation of the homogeneous AEO interaction is more intuitive and physical. We get the same result using the coupled mode equation for the homogeneous AEO interaction in Section 4.2.

Before analyzing the AEO interaction, we briefly

consider AO and EO interactions, and give some formulae for later use. First let's take the AO interaction. As we discussed in previous chapters, the AO effect is an interaction between optical and acoustic waves inside the crystal. The acoustic wave comes from collective molecular displacements of the material. A piezoelectric transducer generates an acoustic wave when we apply the electrical signal to the electrode. If we glue the transducer onto the crystal, we can launch the acoustic wave inside the crystal. Next, the incident optical wave interacts with the acoustic wave, and it is diffracted into many higher-order waves. The AO effect is nonlinear if the input to the system is considered to be the acoustic wave and the output the diffracted light. Thus if we have many acoustic waves inside the crystal, we have harmonic optical plane waves as well as intermodulation waves. The perturbation in polarization due to the AO interaction is given by :

$$\Delta P_i = -\epsilon_0 \epsilon_{il} \epsilon_{jkl} P_{lmn} S_{mn} E_j, \quad (4.1.1)$$

where ϵ_{ij} is the dielectric tensor of the unperturbed medium. If we assume one plane acoustic wave, the strain becomes :

$$S_{mn} = s_{mn} \exp[j(\Omega t - K_i x_i)], \quad (4.1.2)$$

where s_{mn} : constant acoustic strain amplitude,

Ω : acoustic wave frequency,

K_i : acoustic wave vector.

We assume that the amplitude of the acoustic wave does not change as it interacts with the optical wave. Then we can use one grating coupled mode equation to analyze the AO interaction. From the general coupled mode equation, we see that two mode coupling equation becomes as follows, assuming Bragg diffraction :

$$\begin{aligned} dF^{(0,1)} &= jkF^{(1,2)}\exp[j\Delta kr] \\ dF^{(1,2)} &= jk^*F^{(0,1)}\exp[-j\Delta kr], \end{aligned} \quad (4.1.3)$$

where d is a differential operator with respect to r , and k is a coupling coefficient.

The solution of (4.1.3) with the boundary condition $F^{(0,1)}(0) = 1$, $F^{(1,2)}(0) = 0$ is given by:

$$I_d = I_{in} \eta [\text{sinc}\{\eta + (\Delta kL/2)^2\}^{1/2}]^2, \quad (4.1.4)$$

where η : diffraction efficiency,

L : interaction length,

Δk : phasemismatch.

(4.1.4) is the fundamental formula with which we can calculate the bandwidth of the AO modulator, the number of resolvable spots of the AO deflector, or the wavelength range of the optical filter and spectrum

analyzer.

The linear EO effect comes from the interaction of the low-frequency electric field and optical wave. The effect is given by :

$$\Delta P_i = -\epsilon_0 \epsilon_{il} \epsilon_{jk} r_{lkm} E_m^{(ext)} E_j. \quad (4.1.5)$$

The general expression of the modulated light intensity with cross polarizers is :

$$I_d = I_{in} [\sin(|J(1,2)|r)]^2, \quad (4.1.6)$$

where $|J(1,2)| = (1/2)(\omega/c)(n^{(1)}n^{(2)})^{-1/2}(\epsilon_{il}\epsilon_{jm})$
 $\times |e_i^{(1)} r_{lmk} e_j^{(2)} E_k^{(ext)}|$.

This is the basic formula for the EO device.

In this section, we introduce the homogeneous AEO interaction. In the following sections, we show how to improve the AO deflector, and make a new AEO modulator using the constant AEO interaction. These will exemplify the new possibility of using the simplest combined interaction of AO and EO effects.

4.2. Coupled mode analysis of the homogeneous AEO interaction

As explained above, the perturbation in the dielectric tensor for the homogeneous AEO interaction is

the sum of those of AO and EO effects. Thus, this is given by :

$$\varepsilon_{ij} = \varepsilon_{ij}^{(0)} + \Delta\varepsilon_{ij}^{(AO)} + \Delta\varepsilon_{ij}^{(EO)}, \quad (4.2.1)$$

$$\text{where } \Delta\varepsilon_{ij}^{(AO)} = -\varepsilon_{ip}\varepsilon_{jq}d_{ppqkl}S_{kl},$$

$$\Delta\varepsilon_{ij}^{(EO)} = -\varepsilon_{ip}\varepsilon_{jq}r_{pqk}E_k^{(ext)}.$$

In general, we may have a polarization perturbation which is a product of those for AO and EO effects. But this is a higher order perturbation, and small. Thus we neglect the product effect of AO and EO interactions. The incident optical wave is assumed to be an eigenmode of the unperturbed material with polarization 1 :

$$E_i^{(0,1)}(x,t) = (n^{(0,1)})^{-1/2} e_i^{(0,1)} \times \exp[j\omega^{(0)}\{(n^{(0,1)}r/c) - t\}], \quad (4.2.2)$$

where $r = s_i x_i$ and s is the unit vector in the direction of propagation of the incident light wave.

We assume that the acoustic wave is a plane wave :

$$u_i(x,t) = U_i \exp[j(\Omega t - K_1 x_1)] + \text{c.c.}, \quad (4.2.3)$$

where U_i is the constant amplitude of the plane acoustic wave, and c.c. means complex conjugate.

From the definition of the strain tensor S_{kl} ,

$$S_{kl} = 1/2(D_k(u_l) + D_l(u_k)), \quad (4.2.4)$$

we have the following expression for $\Delta \varepsilon_{ij}^{(AO)}$:

$$\begin{aligned}
 \Delta \varepsilon_{ij}^{(AO)} &= (1/2) j \varepsilon_{ip} \varepsilon_{jq} \rho_{pqkl} (U_l K_k + U_k K_l) \exp[j(\Omega t - K_l x_l)] \\
 &\quad - (1/2) j \varepsilon_{ip} \varepsilon_{jq} \rho_{pqkl} (U_l^* K_k + U_k^* K_l) \exp[-j(\Omega t - K_l x_l)] \\
 &= (1/2) a_{ij} \exp[j(\Omega t - K_l x_l)] + \text{c.c.}, \quad (4.2.5)
 \end{aligned}$$

where $a_{ij} = j \varepsilon_{ip} \varepsilon_{jq} \rho_{pqkl} (U_l K_k + U_k K_l)$.

As we see in (4.2.1), we have two perturbations induced by AO and EO effects. If we have two perturbations, we need a two-dimensional integer set to describe the eigenmodes coupled by perturbations as seen in Section 3.4. But for the case of a homogeneous AEO interaction, one of two perturbations, i.e., EO effect, is homogeneous, and we need only a one-dimensional integer set to describe coupled eigenmodes due to the AO effect. Thus our trial solution reads as follows :

$$\begin{aligned}
 E_i(x, t) &= F^{(I, p)}(r^{(I)}) (n^{(I, p)})^{-1/2} e_i^{(I, p)} \\
 &\quad \times \exp[j\omega^{(I)}(n^{(I, p)} r^{(I)} / c - t)], \quad (4.2.6)
 \end{aligned}$$

where $r^{(I)} = s_i^{(I)} x_i$.

If we use the same approximations as used in Section 3.4, we get the coupled mode equation for the constant AEO interaction :

$$dF^{(I, q)}$$

$$\begin{aligned}
&= H(I, q, p) F^{(I, p)} \exp[j(\omega^{(I)} / c)(n^{(I, p)} - n^{(I, q)})r] \\
&+ J(I, q, p) F^{(I+1, p)} \exp[j(\omega^{(I)} / c)(\Delta k^{(I+1, p)} - \Delta k^{(I, q)})r] \\
&+ J(I, q, p) F^{(I-1, p)} \exp[j(\omega^{(I)} / c)(\Delta k^{(I-1, p)} - \Delta k^{(I, q)})r],
\end{aligned}
\tag{4.2.7}$$

where

$$\begin{aligned}
H(I, q, p) &= (j/2)(\omega/c)(n^{(I, q)} n^{(I, p)})^{-1/2} \\
&\quad \times e_1^{(I, q)} \Delta \varepsilon^{(EO)}_{lm} e_m^{(I, p)}, \\
J(I, q, p) &= (j/4)(\omega/c)(n^{(I, q)} n^{(I+1, p)})^{-1/2} \\
&\quad \times e_1^{(I, q)} a_{lm} e_m^{(I+1, p)}, \\
J(I, q, p) &= (j/4)(\omega/c)(n^{(I, q)} n^{(I-1, p)})^{-1/2} \\
&\quad \times e_1^{(I, q)} a_{lm}^* e_m^{(I-1, p)},
\end{aligned}$$

and d is a differential operator with respect to r .

Let's look at (4.2.7) in detail. The mode of order I couples with eigenmodes of orders I , $I+1$, $I-1$ with respective phasemismatches. In Section 3.4, we saw that the rule of modes coupling is $\Delta I = \pm 1$. But here, in addition to $\Delta I = \pm 1$, we also have a self-coupling $\Delta I = 0$. The fact that one of the perturbations is homogeneous reduces to the self coupling with selection rule $\Delta I = 0$. (4.2.7) is the basic equation which can be used to analyze the general homogeneous AEO interaction. Here, we didn't use a specific form of optical, acoustic eigenmodes, or interaction geometries. (4.2.7) does not allow an analytic solution in general because of the phasemismatch factors. But if the interaction length is

large enough so that only two modes couple with each other, we can obtain an analytic solution. In this case, the general equation (4.2.7) reduces to :

$$\begin{aligned} dF^{(0,1)} &= H(0,1,1)F^{(0,1)} + J(0,1,2)F^{(1,2)} \exp[j\Delta k r] \\ dF^{(1,2)} &= H(1,2,2)F^{(1,2)} + J(1,2,1)F^{(0,1)} \exp[-j\Delta k r], \end{aligned} \quad (4.2.8)$$

where $\Delta k = \Delta k^{(1,2)}$.

We can introduce new amplitudes :

$$\begin{aligned} G^{(0,1)} &= \exp[-H(0,1,1)]F^{(0,1)} \\ G^{(1,2)} &= \exp[-H(1,2,2)]F^{(1,2)}. \end{aligned} \quad (4.2.9)$$

Then (4.2.8) becomes :

$$\begin{aligned} dG^{(0,1)} &= J(0,1,2)G^{(1,2)} \exp[j(\Delta k + q_2 - q_1)r] \\ dG^{(1,2)} &= J(1,2,1)G^{(0,1)} \exp[-j(\Delta k + q_2 - q_1)r], \end{aligned} \quad (4.2.10)$$

where $q_1 = H(0,1,1)/j$, $q_2 = H(1,2,2)/j$.

Next let us define the total phasemismatch Δk_T as :

$$\Delta k_T = \Delta k + (q_2 - q_1). \quad (4.2.11)$$

As we see in (4.2.11), the total phasemismatch consists of the phasemismatch due to the AO effect and that due to the EO effect; i.e., $q_2 - q_1$.

Let us define the phase mismatch due to EO effect as :

$$\Delta k_{EO} = q_2 - q_1$$

$$\begin{aligned}
&= -(1/2)(2\pi/\lambda)(n^{(1,2)})^{-1} \\
&\quad \times \varepsilon_{1i} \varepsilon_{mj} e_l^{(1,2)} r_{ijk} e_m^{(1,2)} E_k^{(ext)} \\
&+ (1/2)(2\pi/\lambda)(n^{(0,1)})^{-1} \\
&\quad \times \varepsilon_{1i} \varepsilon_{mj} e_l^{(0,1)} r_{ijk} e_m^{(0,1)} E_k^{(ext)}.
\end{aligned} \tag{4.2.12}$$

If we define changes of indices of refraction of modes 1,2 due to the EO effect as ,

$$\begin{aligned}
\Delta n_1 &= (1/2)(n^{(0,1)})^{-1} \\
&\quad \times \varepsilon_{1i} \varepsilon_{mj} e_l^{(0,1)} r_{ijk} e_m^{(0,1)} E_k^{(ext)} \\
\Delta n_2 &= (1/2)(n^{(1,2)})^{-1} \\
&\quad \times \varepsilon_{1i} \varepsilon_{mj} e_l^{(1,2)} r_{ijk} e_m^{(1,2)} E_k^{(ext)},
\end{aligned} \tag{4.2.13}$$

then (4.2.12) becomes :

$$\Delta k_{EO} = (2\pi/\lambda)(\Delta n_1 - \Delta n_2). \tag{4.2.14}$$

The initial condition is given by:

$$G^{(0,1)}(0) = 1, G^{(1,2)}(0) = 0. \tag{4.2.15}$$

The solution of (4.2.10) with initial conditions given by (4.2.15) is :

$$\begin{aligned}
G^{(0,1)} &= -j(4|J(0,1,2)|^2 + (\Delta k_T)^2)^{-1/2} \exp[j\Delta k_T r] \\
&\quad \times [C_+ \exp(C_+ r) - C_- \exp(C_- r)] \\
G^{(1,2)} &= jJ(0,1,2)^* (4|J(0,1,2)|^2 + (\Delta k_T)^2)^{-1/2}
\end{aligned}$$

$$x \exp[-1/2j\Delta k_{\text{T}}r] 2j \sin[4|J(0,1,2)|^2 + (\Delta k_{\text{T}})^2]^{-1/2} r], \quad (4.2.16)$$

where $C_{\pm} = 1/2[-j\Delta k_{\text{T}} \pm j(4|J(0,1,2)|^2 + (\Delta k_{\text{T}})^2)^{-1/2}]$.

From (4.2.16), we see that the diffracted light amplitude is given by, at the length $r = L$:

$$\begin{aligned} F^{(1,2)} &= -2J(0,1,2)^* \exp[j(q_2 - 1/2\Delta k_{\text{T}})L] \\ &\quad \times [4|J(0,1,2)|^2 + (\Delta k_{\text{T}})^2]^{-1/2} \\ &\quad \times \sin\{[4|J(0,1,2)|^2 + (\Delta k_{\text{T}})^2]^{1/2} L\}. \end{aligned} \quad (4.2.17)$$

The diffracted light intensity follows :

$$I^{(1,2)} = \eta_{\text{AO}} [\text{sinc}[\eta_{\text{AO}} + (\Delta k_{\text{T}}L/2)^2]^{1/2}]^2, \quad (5.2.18)$$

where $\eta_{\text{AO}} = |J(0,1,2)L|^2$ is the diffraction efficiency of the AO effect in the absence of the EO effect.

If we compare the diffracted light intensity formula for AO and homogeneous AEO interactions, we see that the only difference is the phasemismatch. This was shown in detail in (4.2.12) and (4.2.18). So the physical interpretation of (4.2.18) can be explained as in Fig.4.2.1. If we apply an external electric field, we change the index of refraction. These changes are given by Δn_1 , Δn_2 , which are same as (4.2.13). The phasemismatch for the conventional AO interaction is given from Fig.4.2.1 :

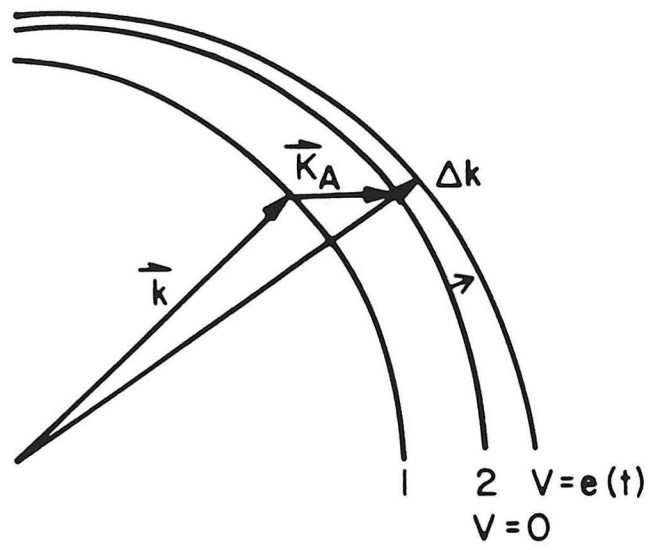


FIG 4.2.1

Fig 4.2.1: Wave vector diagram illustrating the principle of the homogeneous acousto-electro-optic interaction.

Δk : Phase mismatch induced by the homogeneous AEO interaction.

\vec{k}_A : Acoustic wave vector.

$$\Delta k_T = \Delta k + (2\pi/\lambda)(\Delta n_1 - \Delta n_2), \quad (4.2.19)$$

which is the same as (4.2.11).

Then we can directly write down the intensity formula from that of the conventional AO interaction which gives exactly the same formula as (4.2.18).

The above derivation of the formula for the constant AEO interaction using the change of index of refraction is possible only for homogeneous EO effects. If the electric field is spatially varying, we need a two-grating coupled mode equation to analyze the interaction. This subject will be considered in Chapter 5.

4.3. Experimental verification of the homogeneous AEO interaction

The wavevector diagram of the specific interaction geometry we choose for the experiment is shown in Fig. 4.3.1. We considered anisotropic Bragg diffraction. As is shown in Fig.4.3.1, the acoustic frequency has been chosen to give maximum diffracted light intensity without an external voltage. When the external voltage is applied, we introduce phase mismatch, and the intensity of the diffracted light becomes smaller.

The theoretical prediction for this interaction

geometry can be done using the general result derived in Section 4.2. Let us first consider the theoretical diffracted light intensity as a function of the applied external voltage. In Fig. 4.3.1, the acoustic wave travels in the x-direction, and the external voltage is applied in the y-direction. Let the height of the crystal be h . Then the amplitude of the electric field for the given voltage V is :

$$E_2 = V/h. \quad (4.3.1)$$

Next, let us define the voltage V^{AEO} as :

$$\Delta k_T L/2 = \Delta k_{AO} L/2 + \pi V/V^{AEO}. \quad (4.3.2)$$

From (4.2.11) and (4.2.13), we see that V^{AEO} is given by :

$$V^{AEO} = (\lambda h/L) \left[(1/2) (n^{(0,1)})^{-1} \varepsilon_{1i} \varepsilon_{mj} e_l^{(0,1)} r_{ij2} e_m^{(0,1)} - (1/2) (n^{(1,2)})^{-1} \varepsilon_{1i} \varepsilon_{mj} e_l^{(1,2)} r_{ij2} e_m^{(1,2)} \right]^{-1}, \quad (4.3.3)$$

where λ is the wave length of the optical wave and L is the interaction.

For our case, $\Delta k_{AO} = 0$. This gives the intensity formula from (4.2.18) :

$$I_d = \eta_{AO} [\text{sinc}[\eta_{AO} + (\pi V/V^{AEO})^2]^{1/2}]^2. \quad (4.3.4)$$

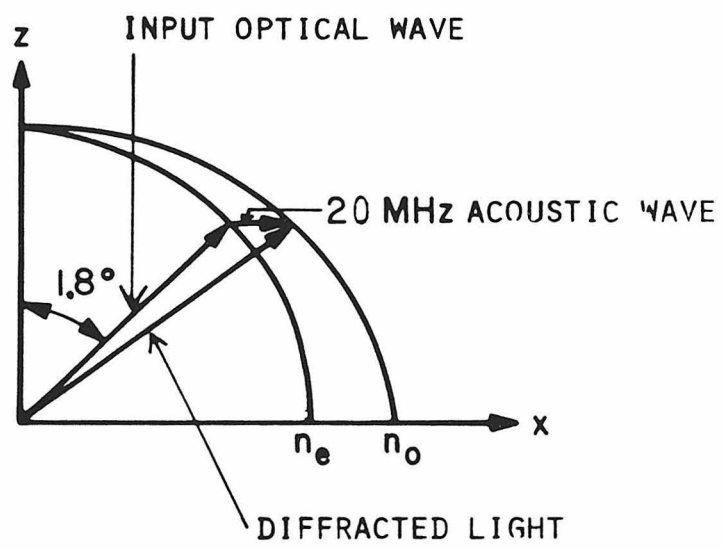


FIG 4.3.1

Fig 4.3.1 : Configuration of the interaction geometry for the AEO light modulation experiment.

n_e : index of refraction of the extraordinary wave.

n_o : index of refraction of the ordinary wave.

This is the theoretical expression of the diffracted light intensity as a function of the applied external voltage for our interaction geometry. If the AO diffraction efficiency is small, as is true for our experiment, (4.3.4) becomes :

$$I_d/\eta_{AO} \sim [\text{sinc}(\pi V/V^{AEO})]^2. \quad (4.3.5)$$

We see from (4.3.5) that if the applied voltage is equal to V^{AEO} , the diffracted light intensity is zero. This shows that the voltage defined in (4.3.3) is the analog of the half-wave voltage for a conventional EO modulator.

For the experimental demonstration of the result (4.3.5), we designed a Bragg cell with electrodes to apply the external voltage. The photograph of the device is shown in Fig. 4.3.2. We chose LiNbO_3 as the crystal of the Bragg cell. As shown in Fig. 4.3.2, the shear acoustic wave with polarization in the y-direction is launched from the transducer glued on the (1,0,0) surface. This acoustic wave propagates in the x-direction, and the center frequency of the acoustic wave was chosen to be 20 MHz. The velocity of the acoustic wave is 4.2×10^5 cm/sec. The input impedance of the transducer was chosen to be 50Ω . Then two metal electrodes were evaporated on the (0,1,0) surfaces and

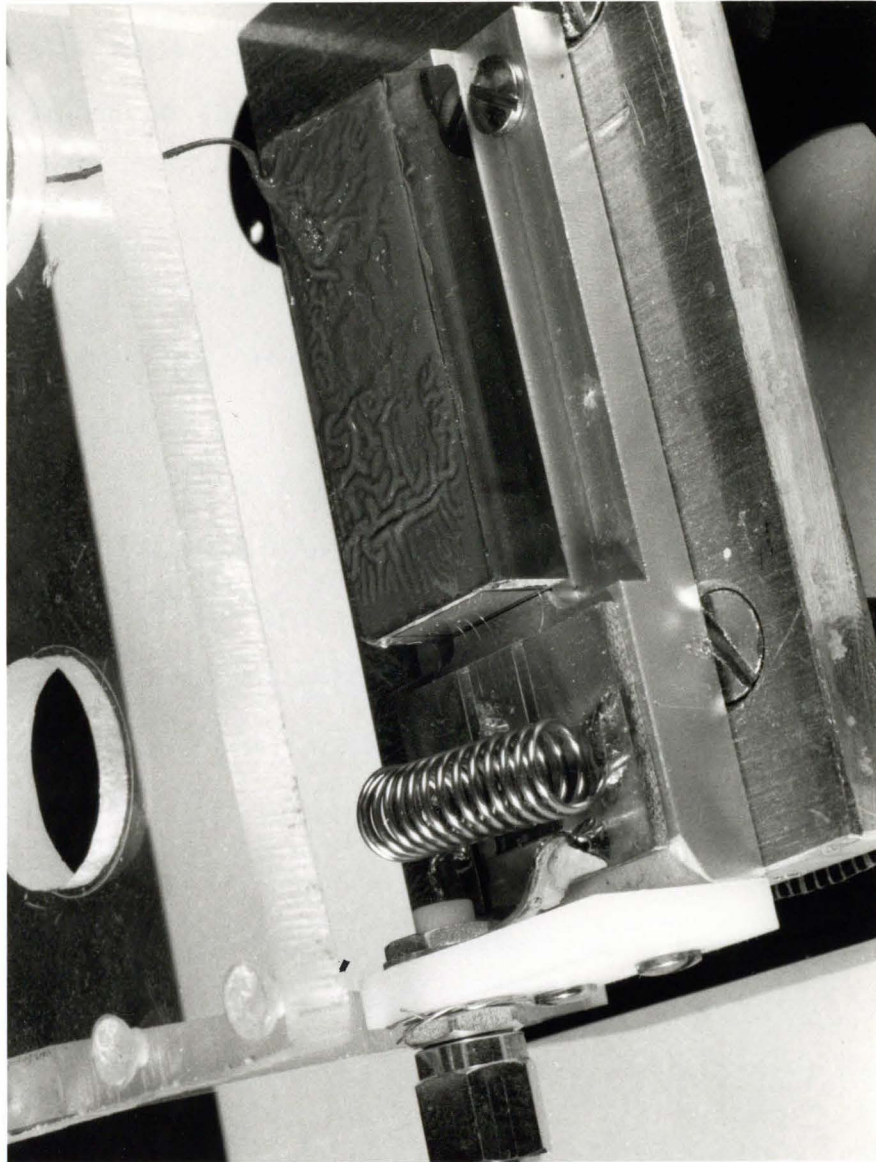


Fig4.3.2

Fig 4.3.2 : Photograph of the device for the AEOLight modulation experiment.

Crystal is LiNbO_3 .

connected to a high-voltage power supply. The specifications of the device are summarized in Table 4.3.1.

We used a 5 mW polarized He-Ne laser as a light source. The input optical wave was polarized in the y-direction, propagating at an angle 1.8 deg with respect to the z-axis. This gives the maximum diffracted light intensity for the 20 MHz acoustic wave. The above angle has been calculated. In the experiment, we illuminated the Bragg cell and rotated it to find the maximum diffracted light intensity. The angle experimentally determined is the same as that calculated. Also, the polarization of the diffracted light was measured and it was in the x-direction. As expected, this interaction was anisotropic. After the Bragg cell, we used a polarizer to block the undiffracted light. This decreased the background light and increased the accuracy of the measurement. A spherical lens with focal length 60 cm was used to focus the output diffracted optical plane wave on a detector.

We measured the maximum diffracted light intensity for the 20 MHz acoustic frequency. Then we increased the external voltage up to 7.5 kV and measured the corresponding diffracted light intensities. We found that at 6 kV the diffracted light intensity was minimum.

Table 4.3.1

Specification of the Bragg cell

- * Crystal : LiNbO_3 .
- * Size of the crystal : 40-7-12(x-y-z) (mm).
- * (0,0,1) surfaces : Polished and A.R. coated.
- * Optical wave : 632.8 nm (He-Ne laser).
- * Acoustic wave : shear wave with a polarization [0,1,0] and propagating in the [1,0,0] direction.
velocity is 4.2×10^5 (cm/sec).
- * Acoustic wave center frequency : 20 ± 5 (Mhz).
- * Diffraction efficiency : 10 (%/watt).
- * R.F. input power : 2 watts.
- * (0,1,0) surfaces : metal electrodes.
- * Size of the transducer : 5-10(y-z) (mm).

This gave $V^{AEO} = 6$ kV. Then we normalized the light intensity and voltage as prescribed in (4.3.5). We plotted the relation, and this experimental result is shown in Fig. 4.3.3. In Fig. 4.3.3, we also drew the theoretical curve which is given by (4.3.5). As we see, the experimental result agrees with the theoretical calculation very well.

We calculated the voltage V^{AEO} for our experiment, using the definition (4.3.3). As shown in Fig. 4.3.1, the light propagates near the z-axis. So the index of refraction is 2.29 for the LiNbO_3 crystal.

From (4.3.3) :

$$V^{AEO} = (\lambda h / L n^3 r_{12}), \quad (4.3.6)$$

where we used $r_{22} = -r_{12}$.

The wavelength of the He-Ne laser is 632.8 nm, and the height of the crystal is 7 mm. The interaction length L is 1 cm, and the electro-optic coefficient r_{12} for the low frequency electric field is 6.7×10^{-12} (m/V). Then, if we plug all numbers into (4.3.6), we get 5.5 kV. This calculation agrees with the experimentally measured value of V^{AEO} within an error. The acousto-optic diffraction efficiency measured was about 2 %. We used the elasto-optic coefficient P_{66} because the acoustic wave with polarization in the y-direction travels in the

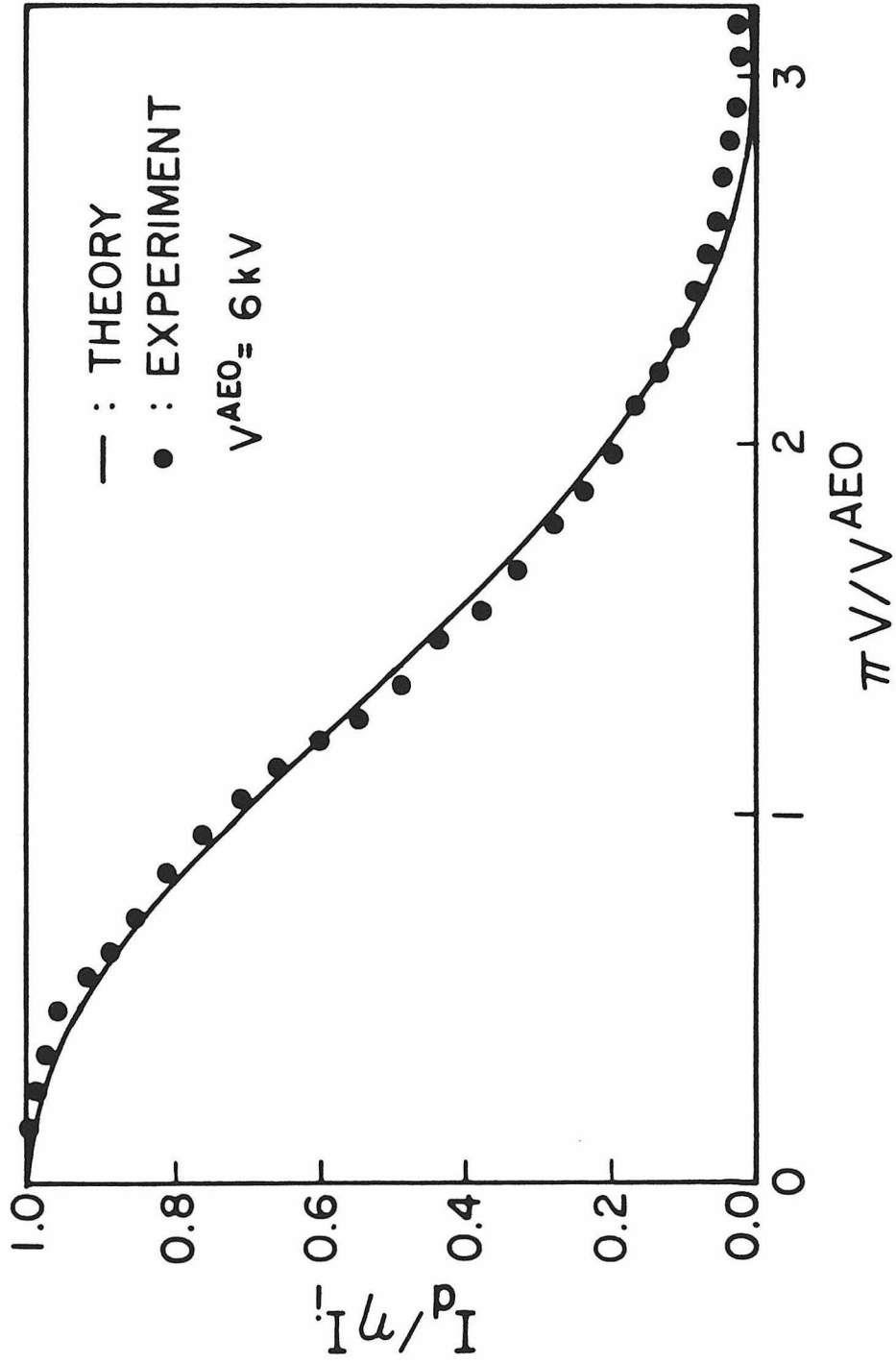


FIG 4.3.3

Fig 4.3.3 : Experimental results of an AEO modulator.

x-direction and polarizations of optical waves are in x- and y-directions. The value of P_{66} for the LiNbO_3 crystal is 0.05. Thus, the diffraction efficiency per unit acoustic power is given by :

$$\eta/P_a = \pi/2^{1/2} \lambda (n^6 P_{66} / \rho V_a^3)^{1/2} (L/h)^{1/2}, \quad (4.3.7)$$

where ρ is the mass density of the LiNbO_3 , which is 4.7810 kg/m³; V_a is the acoustic velocity. If we plug numbers into (4.3.7), we get 7.5%. This result also agrees well with the experiment.

4.4. AEO modulator

The most widely used methods for wideband light modulation are either AO or EO effects. Each type of modulator has its own strength, and suffers from its own distinct limitations. We explain about these in this section in detail when we compare the AEO modulator with AO and EO modulators. When we use AO and EO effects simultaneously, a new flexibility is introduced with which we can overcome some of limitations of two individual modulators.

Let me first consider AO and EO modulators separately. The AO light modulation has been described in Section 4.1. Within the bandwidth of the AO modulator, we can neglect the phase mismatch. Then the

modulation function is given from (4.1.4) :

$$I_d = I_{in} [\sin \eta^{1/2}]^2. \quad (4.4.1)$$

The diffraction efficiency η is proportional to the acoustic power. And the acoustic power is given by :

$$P_a = V^2 / 2R, \quad (4.4.2)$$

where V is the amplitude of the signal voltage, R is the impedance of the electrical network of the acoustic transducer.

From (4.4.1) and (4.4.2), we see that the amplitude modulation function is given by :

$$E_d = E_{in} \sin[aV], \quad (4.4.3)$$

where a is a constant. If the signal is small, we have :

$$E_d \sim V \quad (4.4.4)$$

Thus, if the nonlinear effect which gives rise to harmonic and intermodulations is small, we get the modulation according to (4.4.4). In the following, we call (4.4.1) the modulation function of an AO modulator.

The formula for the EO modulator has been given in (4.1.6). There are two different types of EO modulators. One is the longitudinal EO modulator for which the

electric field is applied in the direction of the light propagation. In this case, the electric field is given by $E = V/L$, where L is the interaction length. From (4.1.6), the modulation function for the longitudinal EO modulator becomes :

$$I_{\text{out}} = [\sin(f(V))]^2 \quad (4.4.5)$$

where $f(V) = (1/2)(\omega/c)(n^{(1)}n^{(2)})^{-1/2} \epsilon_{li} \epsilon_{mj}$
 $\times |e_l^{(1)} r_{ijk} e_m^{(2)} e_k^{(\text{ext})}| V$, and
 $e_k^{(\text{ext})}$ is the direction of the external electric field.

If we apply the electric field in the transverse direction from the light propagation, we have a transverse EO modulator. In this case, the electric field is given by V/h , where h is the height of the transverse dimension. Then the modulation function is given by :

$$I_{\text{out}} = [\sin(g(V))]^2, \quad (4.4.6)$$

where $g(V) = (1/2)(\omega/c)(n^{(1)}n^{(2)})^{-1/2} \epsilon_{li} \epsilon_{mj}$
 $\times |e_l^{(1)} r_{ijk} e_m^{(2)} e_k^{(\text{ext})}| VL/h$.

As we see from (4.4.5), the diffracted light intensity for the longitudinal EO modulation does not depend on the interaction length L . But for the transverse EO modulation, it depends on the ratio L/h , and this gives

some flexibility to design a better modulator. Let's define the half-wave voltages which give the voltages required for the full modulation :

$$f(V) = \pi V/2V_{\pi}^L \quad g(V) = \pi V/2V_{\pi}^T. \quad (4.4.7)$$

From (4.4.5) and (4.4.6) the half-wave voltages are :

$$V_{\pi}^L = [(1/\pi)(\omega/c)(n^{(1)}n^{(2)})^{-1/2}\epsilon_{1i}\epsilon_{mj} \\ \times |e_1^{(1)}r_{ijk}e_m^{(2)}e_k^{(ext)}|]^{-1} \quad (4.4.8)$$

$$V_{\pi}^T = [(1/\pi)(\omega/c)(n^{(1)}n^{(2)})^{-1/2}\epsilon_{1i}\epsilon_{mj} \\ \times |e_1^{(1)}r_{ijk}e_m^{(2)}e_k^{(ext)}|L/h]^{-1}. \quad (4.4.9)$$

In the actual modulation, the signal is biased at $V_{\pi}/2$. Thus the signal becomes :

$$V = V_{\pi}/2 + V_m \sin \omega_m t. \quad (4.4.10)$$

If we plug (4.4.10) into (4.4.5) and (4.4.6), we have :

$$I = 1/2[1 + \sin(\pi V_m \sin \omega_m t / V_{\pi})]. \quad (4.4.11)$$

If we use the Bessel function identities, (4.4.11) becomes :

$$I = (1/2)[1 + 2J_1(\pi V_m / V_{\pi}) \sin \omega_m t \\ + 2J_3(\pi V_m / V_{\pi}) \sin 3\omega_m t + \dots], \quad (4.4.12)$$

where J_n are Bessel functions.

As we see in (4.4.12) the EO modulation creates

nonlinear harmonic frequencies.

AEO light modulation is based on the experimental curve obtained in Section 4.3 for the homogeneous AEO interaction. We use one fixed acoustic frequency which is the center frequency without the external voltage. The acoustic power is constant. Then the input signal for the AEO modulation is the external voltage applied to the device. Thus, we can think of this AEO modulation as the hybrid of AO and EO modulations. The modulation function of the AEO modulator is given by :

$$I = \eta_{AO} [\text{sinc}(\pi V/V^{AEO})]^2. \quad (4.4.13)$$

AEO modulator has some advantages or disadvantages over AO and EO modulators. In the following we compare various characteristics of the AEO modulator with those of AO and EO modulators.

BANDWIDTH : The bandwidth of the AO modulator is limited by the diffraction efficiency. For larger bandwidth we need a small interaction length, which gives effective, small phase mismatch. This can be seen from (4.1.4). But the diffraction efficiency is proportional to the interaction length. Thus, there is a trade-off between the bandwidth and diffraction efficiency for the AO modulator. For the AEO modulator, we use only one fixed acoustic frequency with constant

acoustic power. Thus, we can have arbitrary diffraction efficiency if we choose a large interaction length. The bandwidth of the AEO modulator is thus same as that of the EO modulator. The bandwidth of the EO modulator is given by :

$$\Delta f \sim 1/2\pi R_L C, \quad (4.4.14)$$

where R_L is the shunting resistance and C is the crystal capacitance.

Next, the power needed is proportional to Δf . Thus, the practical bandwidth of the AEO modulator is limited primarily by the maximum power supplied by the electrical driving circuit with which the voltage is applied across electrodes.

DIFFRACTION EFFICIENCY : As discussed in the above for the AEO modulator, the diffraction efficiency depends on the acoustic power supplied by the acoustic port and the interaction length. Thus, there is no trade-off between the diffraction efficiency and bandwidth. Furthermore, the piezoelectric transducer does not affect, unlike the AO case, the bandwidth of the modulator. Therefore, it can be designed to maximize the diffraction efficiency by increasing the transducer width and thus the interaction length.

HALF-WAVE VOLTAGE : Half-wave voltages defined for EO and AEO modulators are measures of the voltage that gives full modulation. We derived expressions for half-wave voltages in (4.4.9) for the transverse EO modulation, and in (4.3.3) for the AEO modulation. From these expressions we see that the voltage level required for the AEO modulator is, within a geometrical factor, close to unity, twice that needed in a transverse EO modulator of the same geometry.

SYSTEM ALIGNING : The modulated light is angularly separated from the undiffracted light, because we used anisotropic AO interactions. Thus, as compared with an EO modulator, the need for an analyzer is eliminated. Furthermore, if we use anisotropic AO diffraction, we don't need the input polarizer either. The alignment of an AEO modulator thus (like an AO modulator) is almost insensitive to the direction perpendicular to the interaction plane. This is to be compared to the small numerical aperture, in both directions, of an EO modulator, limited by the natural birefringence. If we use an analyzer for the anisotropic AO modulator, the signal-to-noise ratio will be enhanced, because polarizations of the diffracted and undiffracted light are orthogonal, and the analyzer suppresses the undiffracted light. The acoustic port can be used to

dynamically align the modulator in the plane of the interaction, by changing the center frequency, and to compensate for the intensity of the acoustic power. The above factors make the system aligning of the AEO modulator very easy compared with the EO modulator.

EXTENDED BEAM MODULATION : For an AO modulator, the modulation is done by the travelling acoustic wave. This means there is an acoustic transit time limit for the AO modulator. But in the AEO modulator the modulation is accomplished not by the acoustic wave but by the voltage. Thus, an extended collimated optical beam can be modulated.

MODULATION DEPTH : The modulation depth of a modulator is defined as :

$$MD = (I_{\max} - I_{\min}) / (I_{\max} + I_{\min}). \quad (4.4.15)$$

For the EO modulator the bias voltage which gives the largest linear region is $V_{\pi}/2$, because the modulation function is $\sin^2(\pi V/2V_{\pi})$. One of the criteria of the linearity of the nonlinear modulation function is the total harmonic distortion (THD). Let's first define THD, using an arbitrary modulation function $E(V(t))$. If we consider a sinusoidal input voltage with bias :

$$V(t) = V_b + V_d \cos \omega t, \quad (4.4.16)$$

the modulated output follows :

$$E(t) = E(V_b + V_d \cos \omega t). \quad (4.4.17)$$

Now $E(t)$ is a periodic function with period $2\pi/\omega$ and even in t . Thus, we can expand $E(t)$ as a Fourier cosine series :

$$E(t) = E^{(n)} \cos n\omega t. \quad (4.4.18)$$

The total average output power is given by :

$$\begin{aligned} I &= \int E^2(t) dt \\ &= 2\pi/\omega [(E^{(0)})^2 + 1/2 \sum_n (E^{(n)})^2]. \end{aligned} \quad (4.4.19)$$

THD is defined as :

$$\text{THD} = 1 - \{1/2(E^{(1)})^2(2\pi/\omega) / (I - (E^{(0)})^2(2\pi/\omega))\}. \quad (4.4.20)$$

The modulation function of an AEO modulator has no obvious bias point because of its sinc^2 nature. Also, it has a second order harmonic. But EO modulator does not generate a second harmonic. Thus, it is difficult to use the ratio of harmonics to compare the linearity. This is the reason why we chose THD to compare the linearities. First, as a reference point, we calculated the THD of an EO modulator, which gives the ratio (first harmonic/third harmonic) 1 %. Then, for various biases we calculated THD's for different ranges of the

modulation voltage. Finally, we chose the bias and voltage range, which gives the maximum MD for the previously fixed THD. The result of the computer calculation shows that the MD for the EO modulator is 48 %, and the MD for AEO modulator is 44 % with bias 1.38. This shows that AEO and EO modulators have almost the same linearity.

4.5. AEO deflector

An optical deflector is a device which can change the direction of light propagation. Among many deflectors AO and EO deflectors are used widely. We can control the deflection angle electrically for both deflectors. In this section we concentrate on the AO deflector. In the AO deflector we change the acoustic frequency to change the deflection angle. But as we have seen, if the acoustic frequency deviates from the center frequency, the deflected light intensity drops. Thus, the total deflected angle depends on the bandwidth of the AO device. One of the important figures of merit of the deflector is the number of resolvable spots. This quantity N_R is defined as :

$$N_R = \Delta\beta / (\lambda/nW), \quad (4.5.1)$$

where $\Delta\beta$ is the total deflected angle inside the

crystal, n is the index of refraction, λ is the optical wavelength in vacuum, and W is the beam width of the optical wave. In (4.5.1) we assumed a collimated optical beam with width W . The diffraction-limited angle of this optical beam is λ/nW . Let's first derive a relation between $\Delta\beta$ and the bandwidth Δf . The general wave vector diagram for an AO deflector is shown in Fig. 4.5.1(a). From the figure we have the following equation which contains $\Delta\beta/2$:

$$(K + \Delta K)^2 = (2\pi n_1/\lambda)^2 + (2\pi n_2/\lambda)^2 - 2(2\pi n_1/\lambda)(2\pi n_2/\lambda)\cos(\beta + \Delta\beta/2), \quad (4.5.2)$$

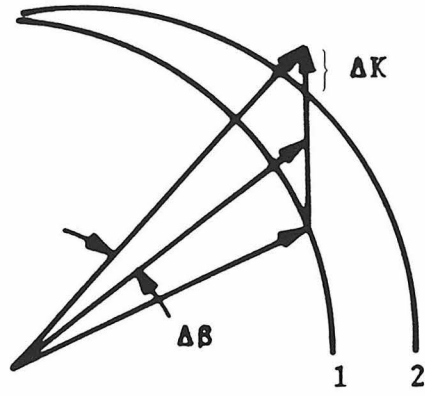
where $\Delta K = 2\pi\Delta f/V_a$ (Δf is the one-sided bandwidth of the device), n_1 and n_2 are indices of refraction for the two polarizations.

From Bragg condition, we have :

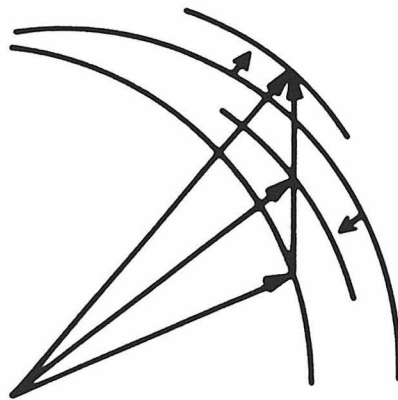
$$K^2 = (2\pi n_1/\lambda)^2 + (2\pi n_2/\lambda)^2 - 2(2\pi n_1/\lambda)(2\pi n_2/\lambda)\cos(\beta). \quad (4.5.3)$$

Here we assume $\Delta\beta/2$ to be small, so that the index of refraction does not change within the angle $\Delta\beta$. Also we assume $\Delta K/K \ll 1$. Then from (4.5.2) and (4.5.3), we have :

$$K\Delta K \sim (2\pi n_1/\lambda)(2\pi n_2/\lambda)(\Delta\beta/2)\sin\beta. \quad (4.5.4)$$



(a)



(b)

FIG 4.5.1

Fig 4.5.1: Wave vector diagram illustrating the phasemismatch compensating AEO deflector.

- (a) Ordinary acousto-optic deflector.
- (b) Phasemismatch compensated AEO deflector.

If we use $|n_1 - n_2|/n_1$ or $n_2 \ll 1$, (4.5.4) becomes :

$$N_R = [W/(V_a \cos(\beta/2))] (2\Delta f), \quad (4.5.5)$$

where $2\Delta f$ is the full bandwidth of the device. (4.5.5) shows that the number of resolvable spots is the product of the bandwidth and the transit time of the acoustic wave across the optical beam.

One method of increasing the number of resolvable spots is to increase the bandwidth of the device. As we have seen in the AEO modulator, there is a trade-off between the bandwidth and diffraction efficiency. Thus it is difficult to increase the bandwidth by decreasing the interaction length. The full bandwidth of the device is determined by the transducer bandwidth and the phasemismatch introduced by the deviation of the scanning acoustic wave frequency from the center frequency. The transducer bandwidth is determined by the electrical matching network of the transducer. But the bandwidth limited by the phasemismatch can be corrected if we change the index of refraction, using the external voltage. This is just the homogeneous AEO interaction. Thus, the AEO deflector is based on the phasemismatch compensation which manifests in the homogeneous AEO interaction.

Let's consider the AEO deflector in detail. For

each scanning frequency f , the phasemismatch $\Delta k_{AO}(f-f_c)$ is introduced as shown in Fig. 4.5.1(b). f_c is the center frequency. The phasemismatch Δk_{AO} is given by :

$$\Delta k_{AO} = [(K + \Delta K)^2 + (2\pi n_2/\lambda)^2 - 2(K + \Delta K)(2\pi n_2/\lambda) \times \cos\alpha]^{1/2} - (2\pi n_1/\lambda), \quad (4.5.6)$$

where $\Delta K = 2\pi(f-f_c)/V_a$, $K = 2\pi f_c/V_a$.

The center frequency satisfies :

$$(2\pi n_1/\lambda)^2 = K^2 + (2\pi n_2/\lambda)^2 - 2K(2\pi n_2/\lambda)\cos\alpha. \quad (4.5.7)$$

From (4.5.6) and (4.5.7), we have :

$$\Delta k_{AO} = (2\pi\lambda f_c/(n_1 V_a^2) - 2\pi n_2 \cos\alpha/(n_1 V_a))(f-f_c) + \pi\lambda(f-f_c)^2/n_1 V_a^2. \quad (4.5.8)$$

From (4.5.8) we see that for small deviation of frequencies, Δk_{AO} is proportional to $(f-f_c)$. The total phasemismatch of the constant AEO interaction follows from (4.2.11) :

$$\Delta k_T = \Delta k_{AO} + 2\pi(\Delta n_1 - \Delta n_2)/\lambda. \quad (4.5.9)$$

If we use (4.5.8) to first order in $(f-f_c)$, we obtain :

$$\begin{aligned} \Delta k_T = & (2\pi\lambda f_c/(n_1 V_a^2) - 2\pi n_2 \cos\alpha/(n_1 V_a))(f-f_c) \\ & + (2\pi/\lambda)((1/2)n_1^{-1} \epsilon_{li} \epsilon_{mj} e_l^{(0,1)} r_{ijk} e_m^{(0,1)} e_k \\ & - (1/2)n_2^{-1} \epsilon_{li} \epsilon_{mj} e_l^{(1,2)} r_{ijk} e_m^{(1,2)} e_k) V/h. \end{aligned} \quad (4.5.10)$$

Now for each frequency we want $\Delta k_T = 0$. Then we get no phasemismatch, and get the maximum diffracted light intensity. From (4.5.10) the relation between the compensating voltage V and the frequency deviation is given by :

$$V = a(f-f_c), \quad (4.5.11)$$

$$\begin{aligned} \text{where } a = & -(2\pi\lambda f_c / (n_1 V_a^2) - 2\pi n_2 \cos / (n_1 V_a)) (\lambda / 2\pi) 2h \\ & \times (n_1^{-1} \epsilon_{1i} \epsilon_{mj} e_l^{(0,1)} r_{ijk} e_m^{(0,1)} e_k \\ & - n_2^{-1} \epsilon_{1i} \epsilon_{mj} e_l^{(1,2)} r_{ijk} e_m^{(1,2)} e_k)^{-1}. \end{aligned}$$

To verify the relation (4.5.11), we did an experiment with the same device as discussed in Section 4.3. The experimental result is shown in Fig. 4.5.2. The normalized intensity of the diffracted light obtained with and without the compensating voltage is plotted as a function of the acoustic frequency. The compensating voltage, as a function of the acoustic frequency, is plotted in the same figure. From Fig. 4.5.2, we can see that the bandwidth of the AEO deflector is about 2.5 times larger than that of the AO deflector and was limited by the electrical bandwidth of the transducer.

Next let's derive the formula of N_R of the AEO deflector, neglecting the influence of the transducer bandwidth. The total number N_R' is given by :

$$N_R' = a(\Delta f + V_{\max} F / V^{\text{AEO}}), \quad (4.5.12)$$

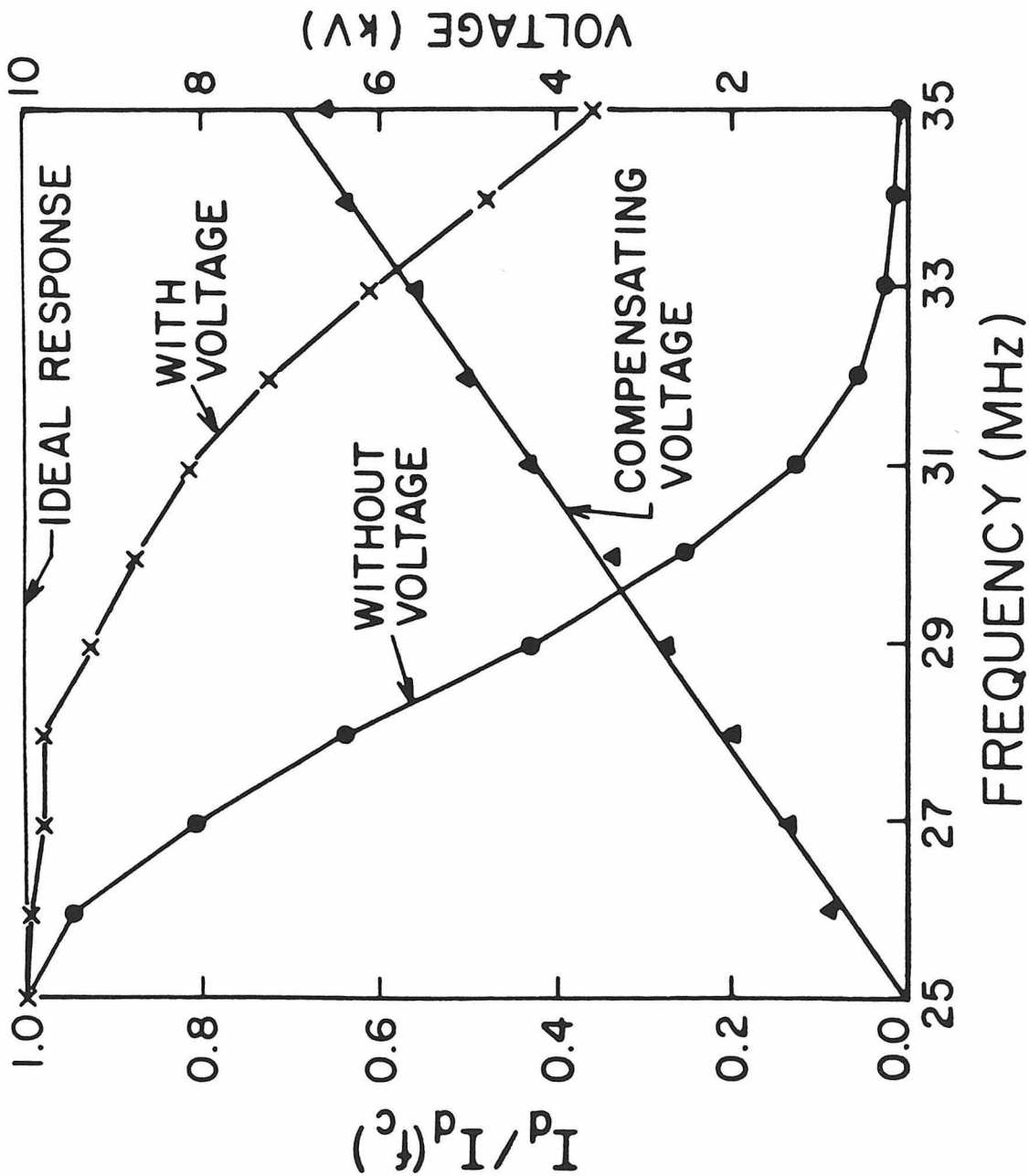


FIG 4.5.2

Fig 4.5.2 : Experimental results of a phasemismatch compensated AEO deflector.

where $\alpha \Delta f = N_R$, Δf is the one-sided bandwidth, F is the whole range of the frequency which compensates the phasemismatch introduced by the voltage V^{AEO} . From (4.5.12) we have :

$$N_R' = N_R(1 + FV_{\max}/(\Delta fV^{AEO})). \quad (4.5.13)$$

The ratio $F/\Delta f$ is given by :

$$F/\Delta f = \pi/\sin^{-1}(2^{-1/2}). \quad (4.5.14)$$

We get the value 2.25 for the above ratio. This finally gives the number of resolvable spots with compensating voltage V_{\max} neglecting transducer bandwidth as :

$$N_R' = N_R(1 + 2.25V_{\max}/V^{AEO}) \quad (4.5.15)$$

4.6. Novel way of measuring the acoustic transducer bandwidth

The transducer bandwidth we discussed in Section 4.5 comes from the impedance mismatch of the electrical network of the transducer. Thus, we can measure this bandwidth, analyzing the transducer network electrically. But from the discussion of the AEO deflector, we can measure this bandwidth optically. In Fig.4.5.2, even if we compensate the phasemismatch, the output light intensity is not uniform. This is because

the acoustic power for scanning frequencies drops due to the impedance mismatch of the transducer network. Also, the diffracted light intensity is proportional to the acoustic power. Thus, if we measure the diffracted light intensity with the electric field compensation, we obtain the transducer bandwidth of the device. As an example, we see the transducer bandwidth in Fig.4.5.2.

5. PHOTOREFRACTIVE AEO INTERACTION

5.1. Spatial AEO interaction

In Chapter 4, we considered homogeneous AEO interactions that allows a clear physical interpretation in terms of the change of index of refraction. Also, it is the simplest type of AEO interaction. But to explore the full potentiality of the AEO interaction, we need to consider spatially varying electric fields as well. The mathematical tool useful in treating this spatial AEO interaction is the two-grating coupled mode equation developed in Section 3.4. In general, we cannot obtain an analytic solution for the two-grating coupled mode equation, if there is a phasemismatch between coupled modes. This is compared with the case of a homogeneous AEO interaction. For the homogeneous AEO interaction, we derive a general solution in the case of Bragg diffraction. For the analysis we choose a specific case of three mode coupling in the next section, and demonstrate the inhomogeneous AEO interaction in Section 5.4.

We need spatially varying electric fields (i.e., gratings) for the inhomogeneous AEO interaction. The photorefractive effect⁹ is a promising method of obtaining spatial electro-optic gratings. If we

illuminate a light intensity pattern on a photorefractive crystal, we can generate a corresponding charge pattern inside the crystal. This charge pattern gives an electric field pattern and EO gratings result from this field pattern via linear electro-optic effect. We can also erase this pattern easily. Thus, we can implement the real time optical signal processing system, using the photorefractive AEO interaction.

In the inhomogeneous AEO interaction we have the freedom to choose arbitrary gratings from different sources. In this case we may use the nonlinearity of the interaction of many gratings. This is contrary to the conventional AO device. We show a way of using the intermodulation term in devising a correlator.

5.2. Three-mode photorefractive AEO interaction

The simplest coupling of eigenmodes through two gratings is three modes coupling. If we assume perfect Bragg matching, we can obtain a simple, general, analytical solution. This is interesting in itself, and furthermore, we can use this analysis to devise a correlator. In this section, we choose a specific configuration of three modes and two gratings, and derive formulae of diffracted light intensities, using

the general two-grating coupled equation given in Section 3.4.

Let's consider the wavevector diagram shown in Fig. 5.2.1. One grating is in the near y-direction, and the other grating is in the x-direction. Thus, the two gratings are almost perpendicular to each other. We have three optical modes. Mode 1 is the incident light wave with polarization 1. This mode 1 interacts with the photorefractive grating isotropically to give the diffracted mode 2. Next, mode 2 interacts with the acoustic grating anisotropically as well as with photorefractive grating to give the diffracted intermodulation light wave(mode 3). We assume that the phasemismatch between mode 1 and the acoustic grating is large so that we have only three mode coupling as shown in the diagram. The coupled mode equation can be written down from Section 3.4 :

$$\begin{aligned}
 dF_1 &= j\mu_{12}^* F_2 \\
 dF_2 &= j\mu_{12} F_1 + j\mu_{23} F_3 \\
 dF_3 &= j\mu_{23}^* F_2,
 \end{aligned}
 \tag{5.2.1}$$

where F_1 , F_2 and F_3 are amplitudes of optical beams and μ_{12} and μ_{23} are coupling coefficients; d is a differential operator with respect to r . As we see in (5.2.1), we have no direct coupling between mode 1 and

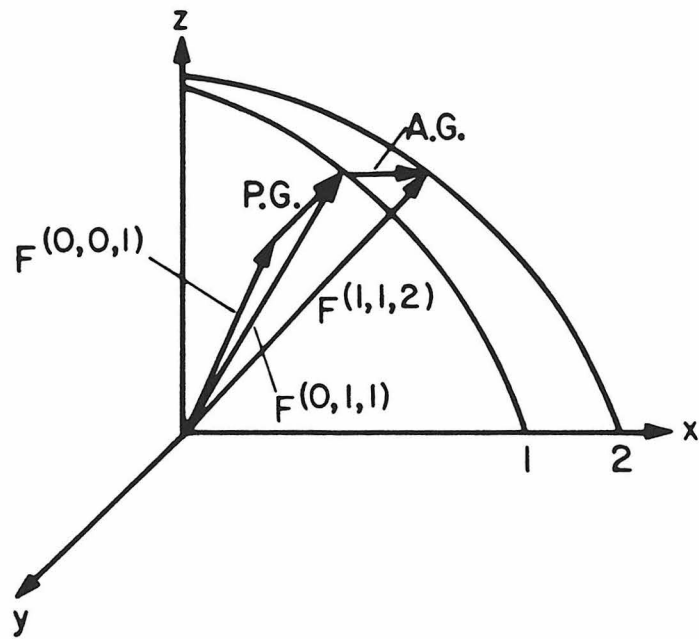


FIG 5.2.1

Fig 5.2.1 : Wave vector diagram of a specific example of photorefractive AEO interaction.

P.G.: photorefractive grating.

A.G. : acoustic grating.

P.G. grating is in y-direction.

$F^{(1,1,2)}$: amplitude of the intermodulation term.

mode 3. This is the consequence of the combined interaction of the two gratings. The initial condition is given by :

$$F_1(0) = 1, F_2(0) = 0 \text{ and } F_3(0) = 0. \quad (5.2.2)$$

The solution of (5.2.1) with initial conditions (5.2.2) is easy to obtain and given by :

$$\begin{aligned} F_1 &= 1 + [|\mu_{12}|^2 / (|\mu_{12}|^2 + |\mu_{23}|^2)] \\ &\quad \times [\cos(|\mu_{12}|^2 + |\mu_{23}|^2)^{1/2} r - 1] \\ F_2 &= [j\mu_{12} / (|\mu_{12}|^2 + |\mu_{23}|^2)^{1/2}] \\ &\quad \times [\sin(|\mu_{12}|^2 + |\mu_{23}|^2)^{1/2} r] \\ F_3 &= [\mu_{12}\mu_{23}^* / (|\mu_{12}|^2 + |\mu_{23}|^2)] \\ &\quad \times [\cos(|\mu_{12}|^2 + |\mu_{23}|^2)^{1/2} r - 1]. \end{aligned} \quad (5.2.3)$$

Let's define diffraction efficiencies η_{12} and η_{23} as :

$$\begin{aligned} \eta_{12} &= (|\mu_{12}|L)^2 \\ \eta_{23} &= (|\mu_{23}|L)^2. \end{aligned} \quad (5.2.4)$$

Then intensities of light waves at $x = L$ are :

$$\begin{aligned} I_1 &= \{1 + \eta_{12} / (\eta_{12} + \eta_{23})\} \\ &\quad \times [\cos(\eta_{12} + \eta_{23})^{1/2} - 1]^2 \\ I_2 &= [\eta_{12} / (\eta_{12} + \eta_{23})] [\sin(\eta_{12} + \eta_{23})^{1/2}]^2 \\ I_3 &= [\eta_{12}\eta_{23} / (\eta_{12} + \eta_{23})^2] [\cos(\eta_{12} + \eta_{23})^{1/2} - 1]^2. \end{aligned} \quad (5.2.5)$$

From (5.2.5) if $\eta_{23} = 0$, we have :

$$I_2 = [\sin\eta_{12}^{1/2}]^2. \quad (5.2.6)$$

This is the well-known formula of the two modes Bragg diffraction. If we have $\eta_{12} = \eta_{23}$ and $(\eta_{12} + \eta_{23})^{1/2} = \pi$; i.e.,

$$\eta_{12} = \eta_{23} = \pi^2/2; \quad (5.2.7)$$

the only nonzero light wave is mode 3, and the intensity is 1. This shows that we can transfer all the incident light energy into mode 3. Also, if we look at the intensity formula of mode 3, it is the product of η_{12} and η_{23} . Thus, we call mode 3 as the intermodulation of two gratings. For small efficiencies:

$$\eta_{12}, \eta_{23} \ll 1. \quad (5.2.8)$$

Then we have approximate light intensities

$$\begin{aligned} I_1 &= 1 \\ I_2 &= \eta_{12} \\ I_3 &= 1/4 \eta_{12} \eta_{23}. \end{aligned} \quad (5.2.9)$$

This is the usual approximation of the undepleted incident light. As we see in (5.2.9), the intermodulation mode is the product of two diffraction efficiencies, when those efficiencies are small. The

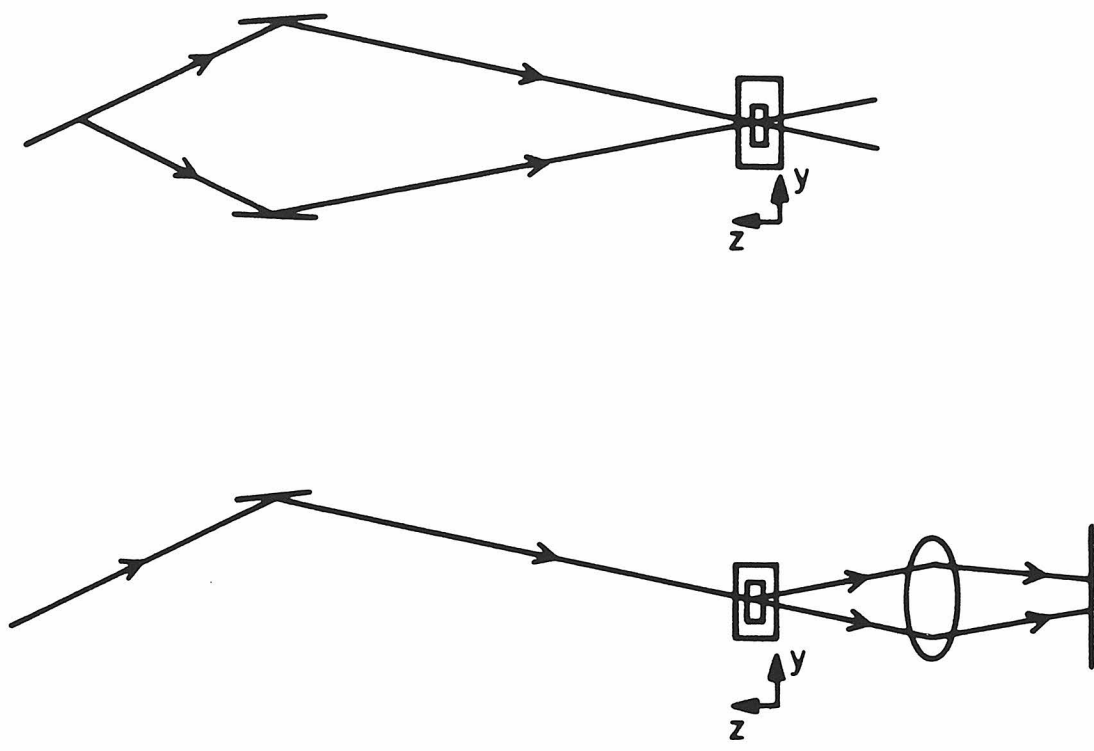
ratio I_3/I_2 is :

$$I_3/I_2 = (1/4)\eta_{23}. \quad (5.2.10)$$

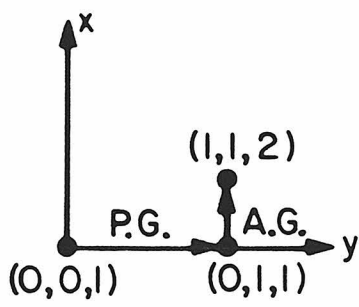
5.3. Experiment on photorefractive AEO interaction

To verify the analysis in Section 5.2, we performed experiments using the device described in Section 4.3. Fortunately, the crystal used for the homogeneous AEO device was LiNbO_3 , and LiNbO_3 is a photorefractive material.

The interaction geometry of photorefractive and acoustic gratings with three optical modes is as shown in Fig. 5.2.1. The interaction geometry of the acoustic wave and optical modes 2 and 3 are the same as that of the experiment of the constant AEO interaction. The experimental setup is drawn in Fig. 5.3.1(a). We used 20 MHz shear acoustic wave. Then we rotated the Bragg cell to obtain the maximum diffracted light intensity. Next we used an Ar laser with blue line (488 nm) to make photorefractive gratings by interfering two collimated blue light beams without the acoustic wave. The power of the laser was 0.7 Watt, and the exposure time was 20 minutes. The angle between the interfering beams was 2.6 degrees. Thus we realized the interaction geometry shown in Fig. 5.2.1. After writing the photorefractive



(a)



(b)

FIG 5.3.1

Fig 5.3.1 : Experiment of the photorefractive AEO interaction.

(a) Writing of the P.G. with two interfering beams without A.G.

AEO interaction given by acoustic wave and the photorefractive grating.

(b) Three spots of the incident, first diffracted and intermodulation lights on the focal plane.

grating, we used one of the blue lights of two interfering beams to obtain the first diffracted light mode 2. Next, we launched the acoustic wave to obtain intermodulation mode 3. After the Bragg cell we used a spherical lens with focal length 60 cm. At the focal plane we observed three spots corresponding to the three optical modes 1, 2 and 3, as illustrated in Fig. 5.3.1(b). Because the acoustic grating is perpendicular to the photorefractive grating, the intermodulation mode 3 is off the line joining the two modes 1, 2. For our experiment the diffraction efficiency η_{12} is the photorefractive diffraction efficiency and it is constant. But we can change the acoustic power and thus can change the diffraction efficiency η_{23} . The dependence of η_{23} on the acoustic power is linear. Thus, the ratio given by (5.2.10) is linear in the acoustic power. We measure the ratio (5.2.10) as we increase the acoustic power. The result is shown in Fig. 5.3.2. In this Figure two scales are arbitrary. For small acoustic power we have a linear relation. For the large acoustic power, however, the relation is not linear. This comes from the saturation of the r.f. amplifier. We also measured two diffraction efficiencies to check the condition (5.2.8). The measured photorefractive diffraction efficiency was 0.6 %, and the maximum

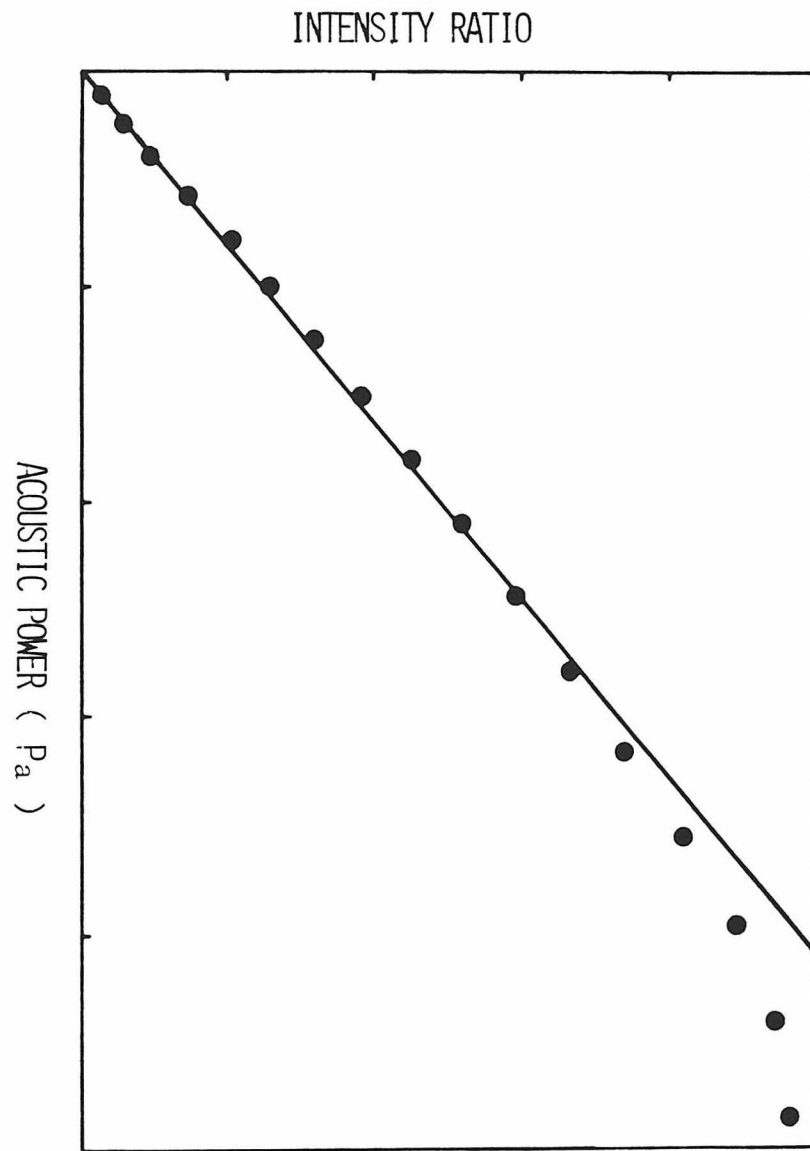


FIG 5.3.2

Fig 5.3.2 : Experimental verification of the photorefractive AEO effect. P_a is the input acoustic power. ● : Experiment.

acousto-optic diffraction efficiency was 0.2.

Let's calculate the change of index of refraction induced by the photorefractive grating. LiNbO_3 , which we used, was not Fe-doped. The diffraction efficiency is given from the paper by F. S. Chen, et al.⁹ as :

$$\eta_{12} = [\sin(\pi\Delta nL/(2\lambda\cos(\alpha/2)))]^2, \quad (5.3.1)$$

where α is the Bragg angle.

For the small diffraction efficiency, we obtain :

$$\Delta n = (2\lambda(\cos(\alpha/2))\eta^{1/2})/(\pi L). \quad (5.3.2)$$

In our experiment, $\lambda = 488 \text{ nm}$, $\alpha = 2.6 \text{ degrees}$ and $\eta_{12} = 0.55\%$. If we plug these numbers in (5.3.2), we obtain $\Delta n = 2 \times 10^{-6}$. This value is in good agreement with the result of F.S.Chen, et al.. Also, this is the saturated value. Next, we calculate the wave number of the photorefractive grating. This is an isotropic grating. Thus we have :

$$\begin{aligned} K &= 2k\sin(\alpha/2) \\ &\sim k\alpha, \end{aligned} \quad (5.3.3)$$

where the approximation is for small α .

If we use $\alpha = 2.6 \text{ degrees}$, we obtain $K = 6 \times 10^3 (\text{cm}^{-1})$. The electric field induced by the photorefractive grating can be calculated, using the following equation :

$$\Delta n = n^3 r_{12} E / 2. \quad (5.3.4)$$

Now $r_{12} = 3.4 \times 10^{-12}$ m/V . We have $E = 10^3$ V/cm.

5.4. Correlator using the intermodulation mode

The mathematical definition of one-dimensional correlation is :

$$\int f(x)h(x-y)^* dx = C(y). \quad (5.4.1)$$

We can do this correlation, using the intermodulation mode of the photorefractive AEO interaction. If the holographic pattern written in the photorefractive crystal is $S(x,y)$, and the acoustic signal delayed in the same crystal is $a(t+x/V_a)$, then the amplitude of the intermodulation mode after the crystal is given by :

$$S(x,y)a(t+x/V_a). \quad (5.4.2)$$

We assumed small diffraction efficiencies and used (5.3.9). After the crystal we can put a cylindrical lens with focal length f . Then on the focal plane the amplitude of the intermodulation mode becomes :

$$\int S(x,y)a(t+x/V_a) \exp[j(\pi x^2 / \lambda f)] dx. \quad (5.4.3)$$

Thus, the intensity distribution on the focal plane is :

$$\begin{aligned}
 I(x_f, t, y) & \\
 &= \left| \int S(x, y) a(t+x/V_a) \exp[jxx_f/\lambda f] dx \right|^2. \quad (5.4.4)
 \end{aligned}$$

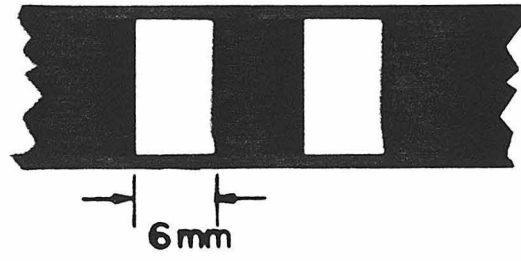
If we use a pinhole detector at $x_f = 0$, we obtain the correlation between $S(x, y)$ and $a(t+x/V_a)$:

$$I(x_f = 0, t, y) = \left| \int S(x, y) a(t + x/V_a) dx \right|^2. \quad (5.4.5)$$

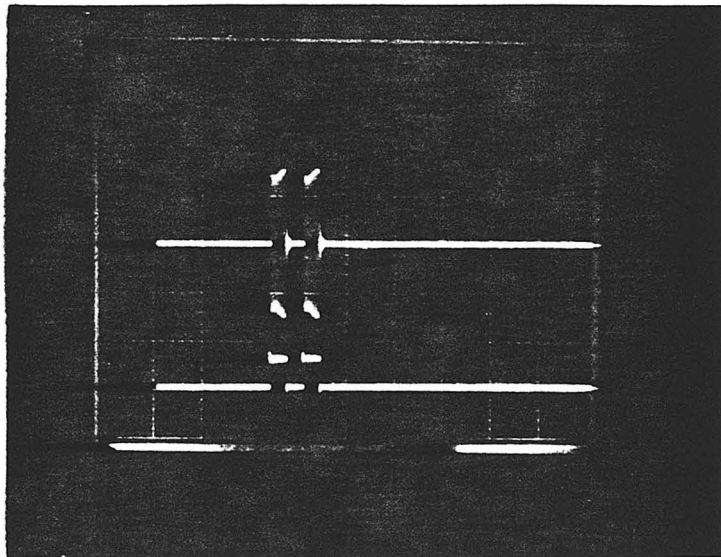
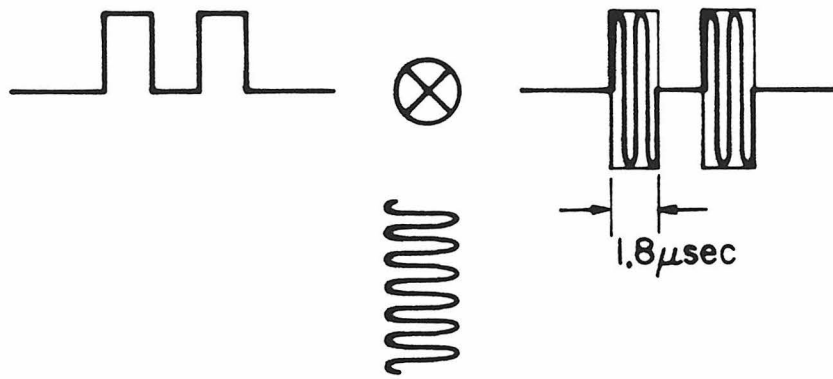
If we collect all the intensity, we obtain the incoherent correlation :

$$\begin{aligned}
 C(t, y) &= \int I(x_f, t, y) dx_f \\
 &= \int |S(x, y)|^2 |a(t+x/V_a)|^2 dx. \quad (5.4.6)
 \end{aligned}$$

To demonstrate the correlation by the above method, we did an auto correlation experiment using the same device as described in Section 4.3. The bandwidth of the device is 10 MHz. Thus, we used the simplest pattern shown in Fig. 5.4.1(a). First, we used a pattern shown in Fig. 5.4.1(a) and two collimated Ar laser beams (488 nm) to write the pattern over the high-frequency interference grating inside the crystal. Of course, the AO device was set before to give the maximum AO diffraction efficiency at the center frequency 20 MHz. Next, we generated an electrical signal which exactly matched the pattern written inside the crystal, when the signal was delayed by the acoustic wave. The electrical



(a)



(b)

FIG 5.4.1

Fig 5.4.1 : Experiment of the photorefractive AEO correlator.

- (a) Input photorefractive pattern. The intensity of the left window is twice that of the right window.
- (b) Electrical signal into the acoustic transducer which matches the pattern (a).
Oscilloscope trace of the electrical signal.

signal was modulated by the center frequency 20 MHz and shown in Fig. 5.4.1(b) and (c). We used a spherical lens with focal length 60 cm and collected all the lights of the intermodulation mode on the focal plane. The oscilloscope trace of the light intensity is shown in Fig.5.4.2. This is the incoherent auto correlation of the pattern shown in Fig. 5.4.1(a).

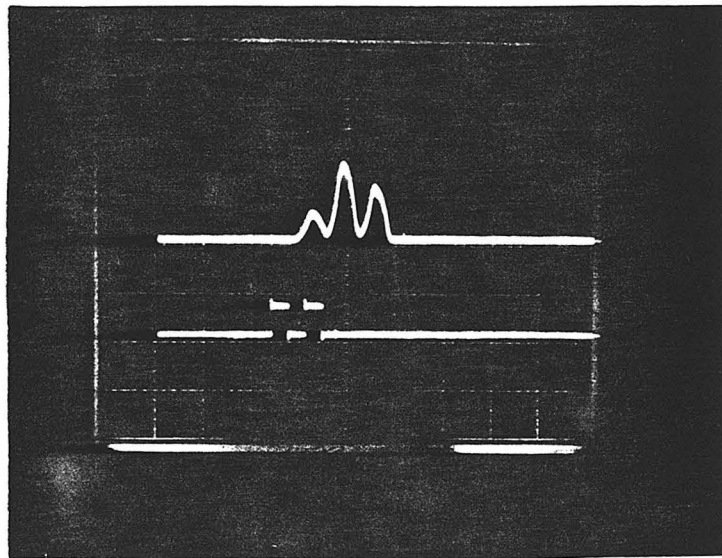


FIG 5.4.2

Fig 5.4.2 : Oscilloscope trace of the auto-correlation of the pattern Fig 5.4.1 (a).

6. FUTURE RESEARCH

In previous chapters, the general concept of multiple perturbations applied to the optical signal processing and optical devices has been developed and demonstrated using the AEO interaction. The main idea of this work was that multiple perturbations might give more flexibilities to play with. This has been demonstrated successfully in Chapters 4 and 5, using the simplest AEO interaction. Thus, if we consider more complicated mutiple perturbations, we may find very interesting phenomena and can apply these phenomena to the optical signal processing and devices.

Small effects of the optical interaction between multiple perturbations is a problem. As we want more flexibility, this problem becomes more severe. There are some ways of overcoming this problem in general. First, we may develop special materials that have large susceptibilities of the interaction of multiple perturbations. People are working on synthetic organic materials, liquid crystals or superlattice of semiconductors to obtain large susceptibilities. Another possibility is to investigate the physical mechanism of the interaction of multiple perturbations. As an example, let's consider AIOHG introduced briefly in Section 2.1. As we discussed in Section 2.1, there are

two types of interactions. One is the direct interaction. The susceptibility of this type of interaction is very small, and we have no way to increase the effect except by developing a special material with a large susceptibility. The second type of interaction is called induced effect. In this case, we have two separate phasematching conditions. One is for the AO interaction, and the other is for the optical second harmonic generation. Thus, if we satisfy two phasematching conditions simultaneously, we obtain a large effect. This has been demonstrated by Nelson and Lax². They increased the effect by order of 1000. This example shows that if we know the physical mechanism of interactions, we may enhance the strength of the interaction. A third way of overcoming difficulties is to control the size of the device, so that for the given value of the susceptibility we can increase amplitudes of multiple perturbations. This gives an overall increased strength of the interaction. Surface acoustic wave device is a good example. In this case, we can increase the amplitude of the strain. Integrated optics is another example. In this case we may have a large electric field, using a small amount of voltage. These are very interesting areas in which to apply the general concept of the interaction of multiple perturbations.

REFERENCES

1. Murray Sargent III, et al., Laser Physics (Addison Wesley, Massachusetts, 1974).
2. D.F.Nelson and M.Lax, Phys.Rev.B 3, 2795 (1971).
3. D.Psaltis, H.Lee and G.Sirat, Appl.Phys.Lett., 46, 215 (1985).
4. I.C.Chang, IEEE Trans.Sonics.Ultrason.SU-23, 2(1976).
5. J.M.Rouaven, M.G.Ghazaleh, E.Bridoux, and R.Torquet, J.Appl.Phys, 50, 5472(1979).
6. D.F.Nelson and P.D.Lazay, Phys.Rev.Lett. 17, 1187 (1970).
7. A.Yariv and Pochi Yeh, Optical waves in crystals : propagation and control of laser radiation (Wiley, NY, 1984).
8. N.Uchida and Y.Ohmachi, J.Appl.Phys. 40, 4692(1969).
9. F.S.Chen, J.T.LaMacchia and D.B.Fraser, Appl.Phys. Lett. 13, 223(1968).